Journal of Hazardous Materials 403 (2021) 123858

Contents lists available at ScienceDirect

Journal of Hazardous Materials

journal homepage: www.elsevier.com/locate/jhazmat

Multisystem combined uranium resistance mechanisms and bioremediation potential of *Stenotrophomonas bentonitica* BII-R7: Transcriptomics and microscopic study

Pinel-Cabello M.[a,*], Jroundi F.[a], López-Fernández M.[b], Geffers R.[c], Jarek M.[c], Jauregui R.[d], Link A.[e], Vílchez-Vargas R.[e], Merroun M.L.[a]

[a] Department of Microbiology, University of Granada, Campus Fuentenueva s/n, 18071, Granada, Spain
[b] Institute of Resource Ecology, Helmholtz-Zentrum Dresden-Rossendorf, Bautzner Landstraße 400, 01328, Dresden, Germany
[c] Genome Analytics, Helmholtz Centre for Infection Research (HZI), 38124, Braunschweig, Germany
[d] AgResearch Grasslands Research Centre, Tennent drive, Palmerston North, New Zealand
[e] Department of Gastroenterology, Hepatology and Infectious Diseases, University of Magdeburg, Leipziger Str. 44.39120, Magdeburg, Germany

ARTICLE INFO

Editor: R. Debora

Keywords:
microbial remediation
RNA-Seq
biosorption
biomineralization
uranium tolerance

ABSTRACT

The potential use of microorganisms in the bioremediation of U pollution has been extensively described. However, a lack of knowledge on molecular resistance mechanisms has become a challenge for the use of these technologies. We reported on the transcriptomic and microscopic response of *Stenotrophomonas bentonitica* BII-R7 exposed to 100 and 250 μM of U. Results showed that exposure to 100 μM displayed up-regulation of 185 and 148 genes during the lag and exponential phases, respectively, whereas 143 and 194 were down-regulated, out of 3786 genes (>1.5-fold change). Exposure to 250 μM of U showed up-regulation of 68 genes and down-regulation of 290 during the lag phase. Genes involved in cell wall and membrane protein synthesis, efflux systems and phosphatases were up-regulated under all conditions tested. Microscopic observations evidenced the formation of U-phosphate minerals at membrane and extracellular levels. Thus, a biphasic process is likely to occur: the increased cell wall would promote the biosorption of U to the cell surface and its precipitation as U-phosphate minerals enhanced by phosphatases. Transport systems would prevent U accumulation in the cytoplasm. These findings contribute to an understanding of how microbes cope with U toxicity, thus allowing for the development of efficient bioremediation strategies.

1. Introduction

Uranium (U) is a naturally occurring radionuclide found as part of minerals such as uraninite (UO_2), pitchblende (U_3O_8), etc. (Selvakumar et al., 2018). Its concentration commonly ranges from 1 to 5 mg/kg in soil, and from 0.1 to 5 μg/L in water (Celik et al., 2018). Anthropogenic activities including U mining, milling and nuclear energy production have increased its concentration to hazardous levels, leading to the contamination of soils, sediments, and waters (Selvakumar et al., 2018). The high persistence of this radionuclide, along with its health and ecological toxicity, underline the need for effective technologies to remediate U pollution. Contamination with U has been associated with renal and liver damage, developmental and reproductive disorders, and DNA damage, being a human carcinogen when its concentration in water exceeds 50 mg/L (Wang et al., 2009; Xu et al., 2018). Conventional remediation approaches may depend on the features of each contaminated environment, and they are expensive, making them difficult to apply accurately. The fact that methods based on chemical and physical techniques can be hard to carry out *in situ* limits their large-scale use. Furthermore, secondary waste forms would be generated due to the employment of chemicals (Gavrilescu et al., 2009). Nowadays, the use of microorganisms as bioremediation agents is seen as an efficient and cost-effective strategy compared to the traditional methods. The benefits of this strategy include the use of native microorganisms from the contaminated site, the transformation in place of the contaminant into a less toxic form, and good environmental regeneration (Selvakumar et al., 2018; Wei et al., 2019). These emerging techniques rely on the use of highly U tolerant microorganisms belonging to

* Corresponding author.
E-mail address: mariapinel@ugr.es (M. Pinel-Cabello).

https://doi.org/10.1016/j.jhazmat.2020.123858
Received 30 April 2020; Received in revised form 18 July 2020; Accepted 24 August 2020
Available online 2 September 2020

bacteria, fungi, algae or yeast (Liang et al., 2016).

In the environment, U exists in many oxidation states —+3, +4, +5 and +6— depending on the geochemical conditions, which control the fate and migration of such radionuclides (Gavrilescu et al., 2009). Most reducing conditions lead to the rapid oxidation of U(III), while U(V) is disproportionate to U(IV) and U(VI), the latter two oxidation states being the most common in nature (Gavrilescu et al., 2009). Under anaerobic conditions, U(IV) precipitates as uraninite, a stable insoluble mineral; under oxidizing conditions, the main U(VI) species is uranyl ion (UO_2^{2+}), held to be the most toxic U species due to its solubility and mobility, in turn highly dependent upon pH. This ion may be absorbed by a mineral surface, precipitated as a phosphate mineral phase, or even form complexes with organic matter over a range of pH below circumneutral values. In the case of alkaline environments, uranyl ions mostly form mobile aqueous complexes with carbonates in groundwaters, increasing U solubility (Beazley et al., 2007).

The ability of a number of bacterial species to use U(VI) as an electron acceptor in anoxic conditions, with the subsequent reduction to an insoluble form of U(IV), has widely been reported —for example, in Fe (III)- and sulphate-reducing bacteria, thermophilic or acidotolerant bacteria (Lakaniemi et al., 2019; Newsome et al., 2014). Li et al. (2017) described this process in *Bacillus* sp. dwc-2, resulting in crystalline accumulations that probably correspond to uraninite phases. Other mineral phases in which U(IV) could precipitate include uramphite [$(NH_4)(UO_2)PO_4{\cdot}3H_2O$] or metaschoepite [$(UO_2)_8O_2(OH)_{12}]{\cdot}10H_2O$, as observed for *Carboxydothermus ferrireducens* and *Shewanella putrefaciens* CN32 (Fredrickson et al., 2000; Slobodkin et al., 2006). Recent studies described the production of noncrystalline U(IV) species both abiotially and biotically, through different mechanisms (Boyanov et al., 2011; Latta et al., 2014), apparently favoured by EPS and biofilms (Bone et al., 2017). Loreggian et al. (2020) studied the stability of noncrystalline U (IV) species in biostimulated sediments under different geochemical conditions, as this form would be more prevalent in the environment. They found that the presence of FeS and reactive oxygen species could lead to a rapid oxidation of tetravalent U in oxic environments, compromising the long-term stability of this approach. The biomineralization of U, resulting in biogenic minerals of U(VI)-phosphate has been found to be a very efficient process of U sequestration over long periods of time (Sowmya et al., 2014; Tu et al., 2019).

The biomineralization of U(VI) mediated by microorganisms has been well documented in recent years (Merroun and Selenska-Pobell, 2008). The interaction of the metal with different metabolites derived from microbial activity (e.g. phosphate) gives rise to the most insoluble form of the metal (Merroun and Selenska-Pobell, 2008). This process, firstly described for the *Citrobacter* genus, was thereafter confirmed in many other bacteria such as *Acinetobacter, Pseudomonas*, *Serratia*, *Sphingomonas* and *Bacillus*, as well as in fungi like *Aspergillus*, *Paecilomyces* or *Rhizopogon* species, and in yeasts (Fomina et al., 2007; Merroun et al., 2011; Tu et al., 2019). Bader et al. (2018) described U biomineralization in the Haloarchaea *Halobacteria noricense* DSM 15987. Phosphatase enzymes expressed by microorganisms are able to efficiently precipitate U(VI) in the presence of organic phosphate sources such as glycerol-2-phosphate (G2P), G3P, phytic acid, or fructose-1, 6-bisphosphate. This leads to the formation of different U (VI)-phosphate minerals —mainly autunite, although chernikovite and ankoleite have also been observed (Beazley et al., 2009; Salome et al., 2017).

Effective bioremediation based on U biomineralization requires an understanding of the mechanisms involved in the bacterial U precipitation, as well as of the response of microorganisms to this radionuclide toxicity. High throughput technologies (e.g. transcriptomic-based approaches) allow for retrieval of great quantities of data regarding biological, molecular and functional processes. The integral analysis of such valuable information sheds light on the response of the entire cellular system under specific conditions. Holmes et al. (2009) performed a transcriptomic analysis of *Geobacter uraniireducens* grown in contaminated sediments from an aquifer in Rifle (Colorado). They described a high expression of genes for energy metabolism, especially those implicated in electron transfer such as c-type cytochromes, and possibly involved in U(VI) reduction. Wang et al. (2019) compared the gene expression between a U(VI)-tolerant strain of *Bacillus atrophaeus* and a sensitive strain of the same species, to determine specific genes that could be involved in U(VI) tolerance. These authors showed the presence of two genes, *ytiB* and *ythA*, encoding for a carbonic anhydrase and a subunit I of cytochrome bd oxidase, respectively, that could have a negative effect on bioremediation of the radionuclide. In another study of U resistance, Dekker et al. (2016) investigated the proteomic response of *Acidithiobacillus ferrooxidans* exposed to 0.5 mM of U(VI). In view of the up-regulated proteins, the authors proposed protection from oxidative stress and U-binding to phosphate compounds as the main mechanisms underlying U tolerance in this bacterium.

The present work focuses on the transcriptional response to U toxicity of a new bacterial species, *Stenotrophomonas bentonitica* BII-R7, isolated from Spanish bentonite clay formations. Previous whole genome analysis of this strain revealed the presence of many genes that confer tolerance to heavy metals, including U and selenium (Se) (Sánchez-Castro et al., 2017a), and grow even in the presence of 6 mM of U (López-Fernández et al., 2014). Here, it is of particular interest to additionally highlight the presence of phosphatase enzymes, previously shown to take part in the biomineralization process of U(VI) to U (VI)-phosphate minerals (López-Fernández et al., 2014; López-Fernández et al., 2015; Sánchez-Castro et al., 2017a). Still, genetic and molecular mechanisms underlying this tolerance remain unknown. The aim of this study was therefore to determine the transcriptomic profile of *S. bentonitica* BII-R7 for the identification of pathways and genes involved in U stress response.

2. Materials and methods

2.1. Bacterial strain and growth conditions

The strain used in this study is a new bacterial species isolated in 2014 from Spanish bentonite formations at "El Cortijo de Archidona, Cabo de Gata" Natural Park (Almería, Spain) and described as *S. bentonitica* BII-R7 (López-Fernández et al., 2014; Sánchez-Castro et al., 2017b). The cells were grown aerobically in Luria-Bertani (LB) medium (tryptone 10 g/L, yeast extract 5 g/L, and NaCl 10 g/L, pH 7.0 ± 0.2) for 24 h at 28 °C in a rotatory shaker at 180 rpm.

2.2. U removal by the cells of S. bentonitica BII-R7

To establish the % of U(VI) removal and the inorganic phosphate (P_i) released by the bacterium, a preinoculum was grown aerobically in liquid LB medium (at a concentration of 10%) at 28 °C under shaking during 24 hours. Afterwards, the cells were harvested by centrifugation (for 10 min at 11,000 rpm), washed twice, and resuspended in NaCl 0.9% (w/v). Aliquots were cultivated in Tris Minimal Medium (TMM) modified from Choudhary and Sar (2011), at an initial Optical Density of 0.05 at 600 nm (OD_{600}) (Genesys 10S UV-Vis; Thermo scientific, MA, USA). TMM consisted of Tris-HCl, 6.06 g; NaCl, 4.68 g; KCl, 1.49 g; NH_4Cl, 1.07 g; Na_2SO_4, 0.43 g; $MgCl_2$, 0.2 g; $CaCl_2$, 0.03 g (pH 7.3-7.4); supplemented with D-(+)-Xylose, 105 mM, as carbon source instead of glucose; β-Glycerol phosphate disodium salt pentahydrate, 1.4 mM; sodium acetate, 15 mM; and tryptone, 0.02% (in 1 L of distilled water). A stock solution of $UO_2(NO_3)_2{\cdot}6H_2O$ was prepared at a concentration of 1 M in 0.1 M of $NaClO_4$. This stock solution was filter-sterilized using nitrocellulose filters of 0.22 μm, then stored at 4 °C. For the treated cells, flasks containing TMM were inoculated with a 24 h-old culture of *S. bentonitica* and amended with U to final concentrations of 100 and 250 μM, respectively. Three biological replicates per treatment and sampling time were performed. In addition, heat-killed cells served as controls in order to verify active elimination of the metal by BII-R7. Cell samples

corresponding to 0, 3.5, 18, 21 and 24 h of incubation were collected by centrifugation at 11,000 rpm during 5 min, and supernatants were stored at -20 °C for further analyses. U speciation in the medium was determined using the software Visual MINTEQ (version 3.1). Xylose and tryptone present in the medium were not considered in the calculations as these organic compounds are not included in the databases of the software.

Residual U(VI) present in the supernatants was measured using the Arsenazo III method, described by Jauberty et al. (2013). To this end, 250 µL of the sample were mixed in 1 mL of Arsenazo reagent and the absorbance was measured at 651 nm after 30-60 s. The concentration of free P_i was determined according to Murphy and Riley (1962), by measuring the absorbance at 850 nm after 30 min of the addition of the reagents.

2.3. Impact of uranium on S. bentonitica BII-R7 growth

To determine the effects of U on the growth rate of *S. bentonitica* BII-R7, the strain was grown in TMM liquid medium amended with 100 and 250 µM. Treatments without U were also carried out as controls. All were incubated at 28 °C under shaking. Aliquots of 1 mL were taken every 3 h from all treatments in order to quantify the bacterial growth by measuring the OD_{600}.

2.4. HAADF-STEM/EDX analyses

Cells treated with 100 and 250 µM of U were harvested after 0, 7, 22, 48 and 72 h of incubation and prepared for microscopic analyses as described in Merroun et al. (2005). The cellular location of U precipitates was determined using high-angle annular dark field scanning transmission electron microscopy (HAADF-STEM, FEI TITAN G22 80-300) combined with energy dispersive X-ray (EDX) spectrometry analyses. Selected-area electron diffraction (SAED) allowed us to characterize the nature of minerals formed. TEM specimen holders were cleaned by plasma prior to STEM analysis to minimize contamination.

2.5. RNA extraction and sequencing

To perform transcriptomic analyses, cultures of *S. bentonitica* were prepared in TMM and treated with U under the conditions described above. Samples corresponding to lag and middle-exponential growth phases were harvested at different incubation times: 1 and 5 h of incubation for untreated cell samples, or 1 and 52 h for treatments with 100 and 250 µM of U. Cells were washed twice in NaCl 0.9% (w/v) and pellets were recovered by centrifuging at 5,000 x *g* for 15 min at 4 °C. RNA extractions were carried out immediately.

Total RNA was extracted from each sample using the RNeasy Bacteria Mini kit (Qiagen, Germany) following the manufacturer's instructions. This extraction method included mechanical lysis of the cells using acid-washed glass beads (212-300 µm; Sigma-Aldrich) in FastPrep® FP120, at 6.5 ms^{-1} of speed for 40 s, done twice with an interval of 5 min between cycles. Contaminating DNA was removed from the obtained total RNA using the TURBO DNA-free kit (Ambion, TX, USA), followed by a clean-up protocol with the RNeasy Bacteria Mini kit. Finally, the extracted RNA was eluted using nuclease-free water and EDTA (1 mM) added to each tube for preservation of the samples. Quantification of extracted RNA was determined by means of a Qubit 3.0 Fluorometer (Life Technology), and the quality was checked on 1.5 % (w/v) agarose electrophoresis gel in 1X TAE buffer.

Samples having an amount of total RNA below 50 ng/µL were concentrated to reach the adequate concentration by the ethanol precipitation method. Briefly, 4 vol. of absolute ethanol and 1 vol. of sodium acetate (3 M, pH 5.2) were added to each sample, and the samples were incubated overnight at -20 °C. Pellets were obtained by centrifuging at 16,000 x g for 30 min at 4 °C, and resuspended in nuclease-free water and EDTA (1 mM). Samples were stored at -80 °C until further analyses.

The quality and integrity of total RNA were checked using an Agilent Technologies 2100 Bioanalyzer (Agilent Technologies; Waldbronn, Germany). The RNA sequencing library was generated from 100 ng total RNA using RiboZerorRNA Removal Kit – Bacteria (Illumina) for rRNA depletion, followed by NEBNext® Ultra™ II Directional RNA Library Prep Kit (New England BioLabs), according to the manufacturer's protocols. The libraries were sequenced on Illumina NovaSeq 6000 using the NovaSeq 6000 S1 PE Reagent Kit (100 cycles) with an average of 24,073,898 reads per RNA sample (a maximum of 33,187,977 and a minimum of 15,829,801 reads).

2.6. Computational processing of the transcriptome samples

A reference for the program BBMap was made using the genes from *S. bentonitica* BII-R7 genome (obtained from GenBank/ENA/DDBJ database) and 191 genomic contigs. This reference was used to generate index files with the BBMap program version 37.90 (sourceforge.net/projects/bbmap/). Using this program, paired-end read files of 14 samples were mapped, producing SAM format files. The program samtools version 1.8 was then used to collect mappings with quality scores higher than or equal to 30. Generation of read counts per gene for each of the quality filtered SAM files was carried out by the mapcount program (https://github.com/mpcox/mapcount). Finally, a Ruby script served to compile the read counts of all samples into a single table with genes as rows and count values as columns.

2.7. Biostatistical analyses

Transcripts were obtained by annotating the genes with Rapid Annotation using the SEED-based method of Subsystem Technology (RAST, version 2.0). SSU and LSU subunits of rRNA were eliminated and mRNA raw data were normalized to transcript per million (tpm) in order to have comparable data. A cut-off was set at 500 tpm and all genes below this value were not considered for further analyses. Several genes with high levels of expression were annotated as hypothetical proteins, for which reason manual annotation was performed with BLAST (Basic Local Alignment Search Tool), and the closest bacterial phylogenetic sequences were selected with a minimal query cover level of 60%. Sequences were aligned in Seaview software (version 4.7) for the phylogenetic tree building.

RNA profiles of each sample were clustered using Past3 v. 3.18 according to the Bray-Curtis similarity index. Genes were grouped according to their function, and differential expression was represented in heatmaps using the gplots package with the heatmap.2 function of R software, and in stacked bars with Explicet version 2.10.5. In addition, an interaction network between genes was derived by calculating the Pearson correlation coefficient in R package reshape2; genes that passed a cut-off between -0.9 and 0.9 were represented in Cytoscape 3.6.0 using the Betweenness Centrality of each node.

Raw sequences were submitted to the European Nucleotide Archive (ENA) under the accession number PRJEB37934.

3. Results and discussion

3.1. Impact of U toxicity on S. bentonitica and quantification of U removal

The impact of U(VI), added as uranyl nitrate at concentrations of 100 and 250 µM, on the growth of *S. bentonitica* BII-R7 cells at different incubation times was determined. Significant differences between the untreated and U(VI)-treated samples were observed (Fig. 1). On the one hand, the untreated cells (control sample) exhibited the typical growth curve characterized by a short lag phase and the presence of exponential (0-16 h) and stationary phases (24-96 h). On the other hand, metal-treated cells showed a lag phase whose duration increased in tandem

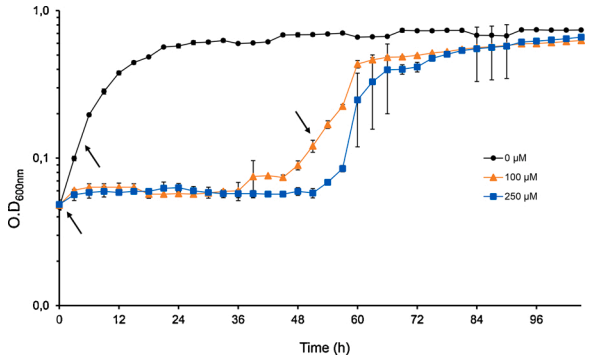

Fig. 1. Growth of *Stenotrophomonas bentonitica* BII-R7 in absence (control) and presence of 100 and 250 µM of uranyl nitrate.

with the metal concentration, i.e. of about 48 h at 250 µM and up to 36 h when cells were exposed to the 100 µM U(VI) initial concentration. In addition, the longer lag phase observed at the 250 µM initial concentration clearly evidenced a higher metal toxicity than the lowest concentration tested. The substantial lag phase found in the present work is most likely related to differential expressions of genes involved in U(VI) tolerance. Many authors have reported variable durations of the lag phase in cells of different bacterial populations treated with U(VI) (Park and Jiao, 2014). For instance, Newsome et al. (2015) observed a lag phase of up to 50 h when *Serratia* species isolated from Sellafield sediments grew in 1 mM of U(VI) under anaerobic conditions.

It is well known that the toxicity of U depends on its oxidation state. While U(VI) is a soluble, mobile and toxic species, insoluble U(VI) species such as U(VI)-phosphate minerals are less toxic and stable (Gavrilescu et al., 2009). In general, the large lag phase exhibited by U-treated cells could be associated with removal of toxic U species from the medium. Therefore, the U removal rate exhibited by the *S. bentonitica* cells at different incubation times was investigated. For this purpose, the cells were grown in TMM amended with 100 and 250 µM of uranyl nitrate, and samples were collected at different incubation times: 0, 24, 48 and 72 h. As the major part of U (93%-96%) was eliminated within the first hours (data not shown), the kinetic of U removal in 24 h of incubation was studied. The amount of the P_i released was also evaluated.

The results indicated that 97% and 96% of U were removed after 24 h of incubation under 100 and 250 µM, respectively (Fig. 2A). A time-dependent increase in the concentration of P_i in the medium was also detected in all treatments, the highest values being obtained under 100 µM of U (Fig. 2B). Differences observed between abiotic controls could be explained by the different initial concentration. The major U species in the TMM (Table 1) are positively charged $(UO_2)_3(OH)_5^+$ and $(UO_2)_4(OH)_7^+$. U removal in the dead biomass is probably due to the sorption of the positively charged metal species to the negatively charged groups of the cell surface. In any case, these values were much lower than those observed with the active cells, suggesting that the U removal is a metabolism-dependent process that probably involves P_i. This is in line with previous results from U removal assays performed with other bacteria. Chandwadkar et al. (2018) showed that *Serratia* sp. strain OT II 7 was able to eliminate up to 94% of 1 mM of uranyl acetate after 24 h of exposure, also with a progressive increase in P_i. Similar levels of U removal were observed in *phoN*-expressing *Deinococcus radiodurans* after 13 h of incubation (Xu et al., 2018).

The exponential growth phase occurred much later than when the concentration of U(VI) decreased. These results suggest that, after U removal, the cells still need some time to grow, most likely to recover from the damage caused by the radionuclide. The stationary phase was reached after 60 and 72 h of incubation, respectively under 100 and 250 µM of U. After this incubation time, however, the toxic effect of U(VI) at both studied concentrations was reduced and the cells reached a final

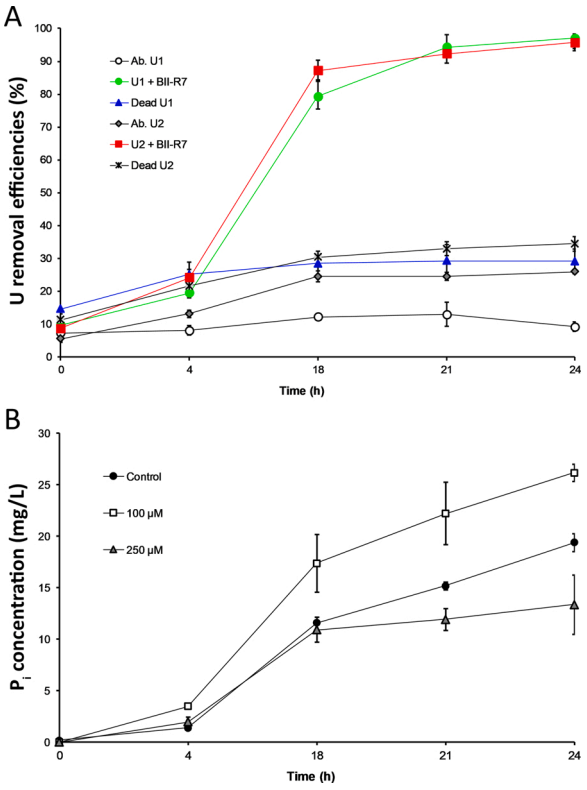

Fig. 2. A. U concentration in the supernatant during the first 24 h of incubation in presence of 100 (U1) and 250 µM (U2) of U. Abiotic (Ab. U1 and Ab. U2) and heat-killed controls (Dead U1 and Dead U2) were performed under the same conditions. B. Concentration in mg/L of the inorganic phosphate (P_i) released by *S. bentonitica* in presence of U.

Table 1
U speciation in the TMM and total concentration of each U species.

% of total concentration		Species name
100 µM	250 µM	
0.383	0.201	UO_2OH^+
0.039	0.027	$(UO_2)_2(OH)_2^{+2}$
60.809	54.793	$(UO_2)_3(OH)_5^+$
37.205	43.945	$(UO_2)_4(OH)_7^+$
0.536	0.483	$(UO_2)_3(OH)_7$-
0.031	0.028	$(UO_2)_3(OH)_4^{+2}$
0.151	0.079	$UO_2(OH)_3$-
0.703	0.368	$UO_2(OH)_2$ (aq)
0.046	0.024	UO_2-(Acetate)$_3$-
0.047	0.024	UO_2-(Acetate)$_2$ (aq)
0.039	0.02	UO_2-Acetate$^+$

cell density (expressed as OD_{600}) relatively similar to that of the untreated cells. Such findings indicated that, despite the low growth rate in presence of U (nearly 4-fold less than that of controls), *S. bentonitica* cells were probably able to develop detoxification strategies to cope with U (VI) toxicity and grow to nearly normal levels.

3.2. HAADF-STEM/EDX analyses

Analyses by STEM of *S. bentonitica* cells treated with 250 µM of U for 22 h (Fig. 3A) revealed that the cell wall may be the main precipitation site of this radionuclide. The amount of U precipitated increased at the longer incubation time, which appeared to be mainly distributed extracellularly as shown in Fig. 3B (48 h). Similar results were obtained when cells were treated with 100 µM of U, where the metal precipitated mostly in the medium surrounding the biomass after 52 h, as shown in

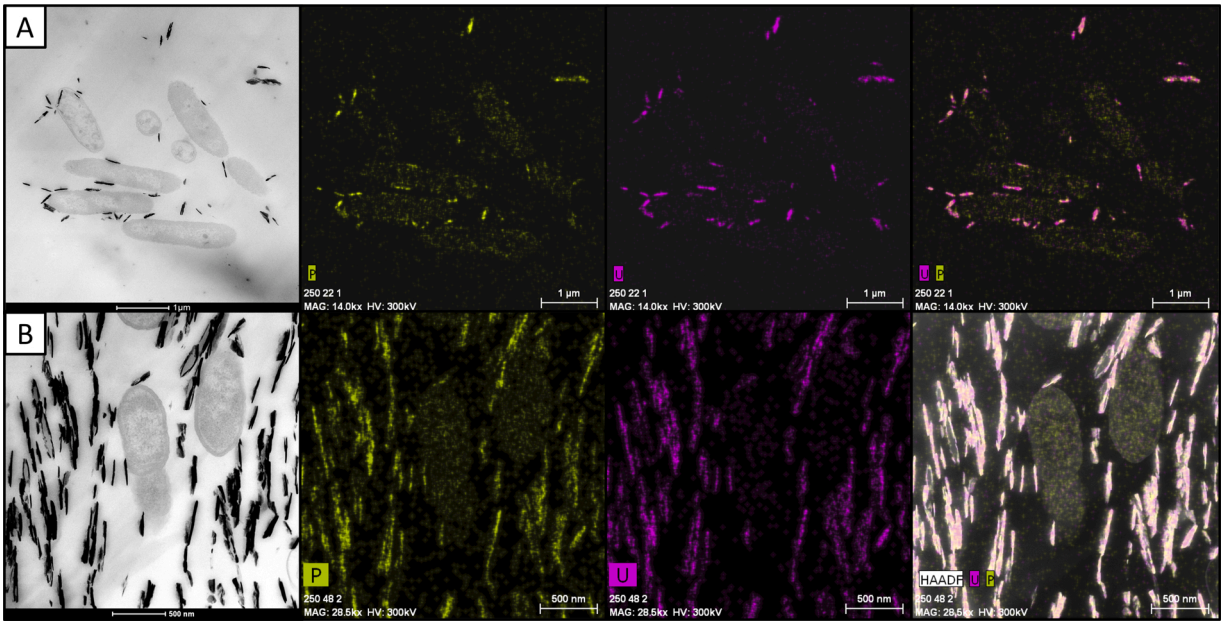

Fig. 3. HAADF-STEM micrographs of extracellular and membrane-associated precipitates formed by *S. bentonitica* after 22 (A) and 48 h (B) of incubation in 250 µM of U. Although RNA samples at these incubation times could not be sequenced, microscopic analysis showed precipitates identical to those formed under 100 µM.

Fig. 4. EDX spectra revealed that the observed electro-dense precipitates were composed of U and P. Selected area electron diffraction (SAED) patterns showed the minerals obtained to be amorphous at both membrane and extracellular levels, although this could be due to the TEM high vacuum (Hu et al., 2005). Interestingly, no intracellular precipitation or accumulation in the treated cells was observed in the studied samples, in contrast with other bacteria (Zhang et al., 2018). The ability of strains of *Stenotrophomonas* genus to bioprecipitate U(VI) has been previously described. Merroun and Selenska-Pobell (2008) reported intracellular deposits of U in *S. maltophilia* JG-2. Furthermore, Islam and Sar (2016) studied the interactions with U of six bacterial species, which showed U precipitates on their surfaces. One of them —related to *Stenotrophomonas* genus (*Stenotrophomonas* sp. U18)— also produced such precipitates extracellularly.

3.3. Transcriptomic analysis

Transcriptomic studies were applied to investigate whether there are any relationships between the large lag phase of cells treated with U(VI) and differential expressions of genes involved in U(VI) tolerance. We focused on gene expression levels obtained during the lag phase (1 h of incubation; time 1) and exponential phase (5 h and 52 h of untreated and metal treated cells, respectively; time 2).

RNA libraries derived from U-treated and untreated cells were constructed for this purpose. Sequencing detected 4191 transcripts, which were aligned with the *S. bentonitica* genome sequence (NCBI Genebank accession number MKCZ00000000.1). On one hand, cells in the lag phase showed up-regulation of 185 genes and down-regulation of 143 under 100 µM of U, while exposure to 250 µM displayed 68 and 290 genes up- and down-regulated, respectively, out of the 3786 genes present in the genome. On the other hand, 148 genes were up-regulated during the exponential phase under 100 µM of U, while 194 were down-regulated. In view of the RNA profiles obtained, Fig. 5 shows the similarities among samples collected at different incubation times. After 1 h of cell incubation, corresponding to the lag phase (Fig. 1), untreated samples form a cluster clearly separate from those under U exposure, showing only 50% of similarity between Uranium and controls. In the exponential phase, controls and uranium did not group separately. These results are in agreement with the growth curves obtained (Fig. 1), supporting the existence of a strong correlation between the gene expression and the sampling times (1 and 52 h).

After 1 h of incubation, significant changes in the gene expression were observed compared to the controls, probably helping the cells cope with the toxicity of U(VI) present in the solution. This similarity in the gene expression observed in the treated and untreated cells in the exponential growth phase (52 h) may be explained by the fact that the metabolic activity at that time was probably more related to simple growth activity than to U depletion or tolerance, which occur in the first hours of the lag phase in the treated cells (Fig. 2A). The high U(VI) removal rate (97%) would help the cells to adapt to metal exposure, resulting in their growth to almost the same level as that of the untreated cells. Consequently, we were interested in investigating the changes occurring in the lag phase, when the difference in gene expression between treated and untreated cells was more than evident as a consequence of the presence of uranium in the medium and the metabolic cell activity to cope with such a toxic radionuclide.

S. bentonitica BII-R7 developed a complex response to U(VI) exposure during lag phase, as shown in Fig. 6. (The complete correspondence of numbers and transcripts are indicated in supplementary table S1). Metal stress caused gene expression similar to that seen in stationary or nutrient-starvation conditions (Hu et al., 2005). We observed down-regulation of genes involved in DNA synthesis and replication (*ribonucleotide reductase class I* and *dnaA*), suggesting important alterations in the cell cycle. Interestingly, expression of *ribonucleotide reductase class I* was negatively correlated with the expression of *phoU*, two *tonB-dependent receptors*, the *RND efflux system*, and *tail-specific protease*, among others. Given that *phoU* is a transcriptional regulator of genes of P metabolism, interactions with a high number of genes could be expected. The same occurred with *tonB-dependent receptors* and the *RND efflux system*. These transcripts form part of protein complexes involved in transport processes, and interactions with other members of the system and membrane proteins, also up-regulated, are essential. *Tail-specific protease* is implicated in the degradation of damaged proteins and the protection from thermal and other stresses.

In addition, chemotaxis and cell motility genes (e.g. flagellar regulatory gene *fleQ*) and those related to cell adhesion, like pilus IV assembly proteins, were down-regulated in all U concentrations. Similar results were obtained for transcripts of aminoacids, carbon metabolism

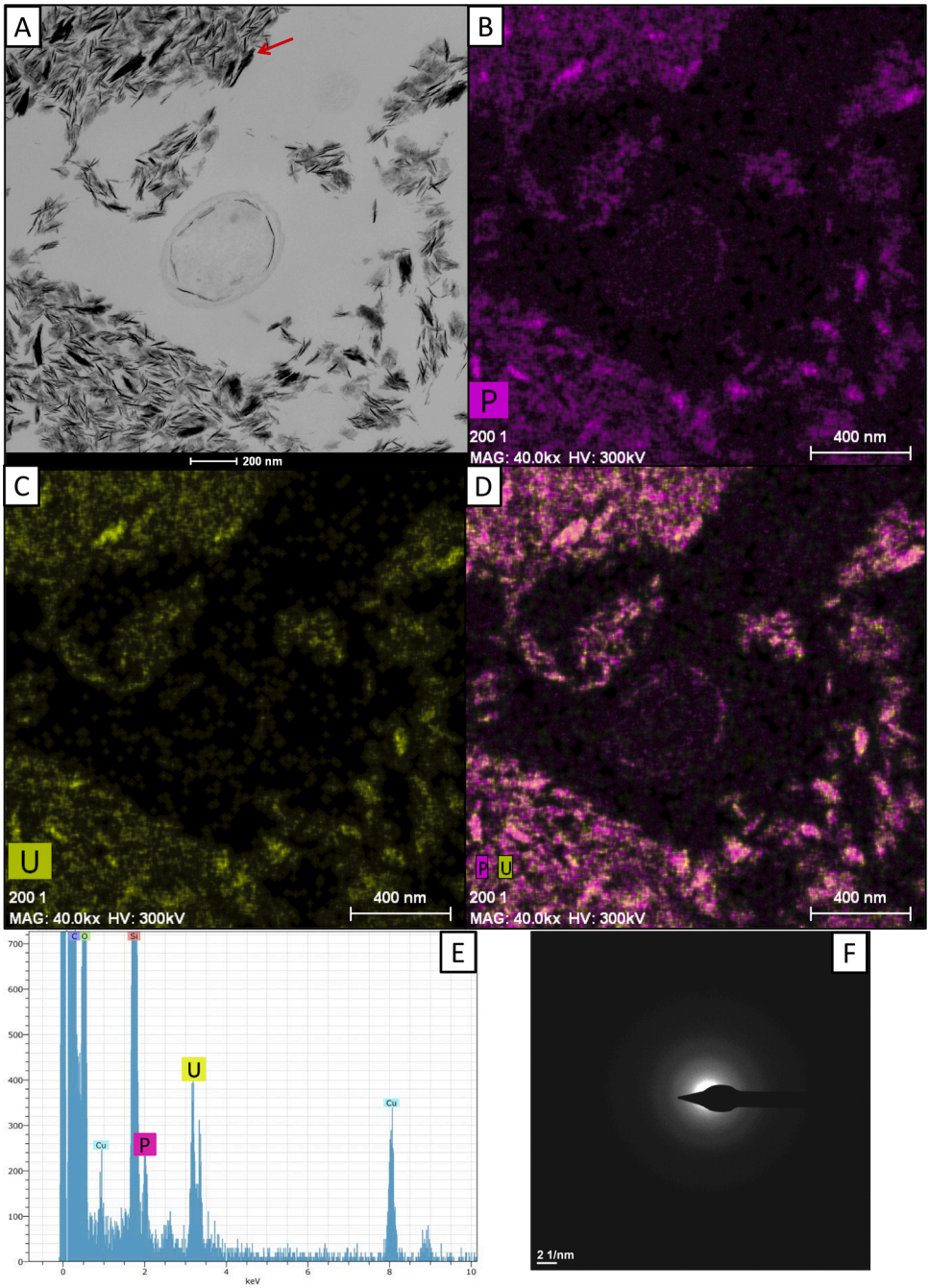

Fig. 4. HAADF-STEM micrographs of *S. bentonitica* cells (A) and element-distribution maps (B, C and D) after 52 h of 100 μM of U exposure. E) EDX analysis showing the presence of U and P in the precipitates. F) SAED pattern of the precipitates.

(e.g. *phenylalanine-4-hydroxylase, aminomethyl transferase, fumaratehydratase*), as well as of lipid metabolism (e.g. *malonyl-CoA transacylase, 3-oxoacyl reductase*) and aerobic oxidative phosphorylation (e.g. *NADH-ubiquinone oxidoreductase, cytochrome O ubiquinol oxidase, succinate dehydrogenase*), especially under 250 μM, showing the higher toxicity of this metal concentration.

These results were in agreement with the effects reported in studies on mutants of *Caulobacter crescentus* exposed to U (Hu et al., 2005; Park and Jiao, 2014). Nevertheless, wild type cells of *S. bentonitica* were able to grow at almost the same level in all tested U concentrations, suggesting the presence of more efficient mechanisms against the toxic effects of this radionuclide. Yung et al. (2014) suggested that the changes in cell cycle were insufficient to produce significant differences in the growth rate, thus explaining the observed growth recovery. Yet in the case of *S. bentonitica*, the lag phase extended about 35 h more, indicating that the down-regulation of cell cycle genes had a strong impact on the growth. We barely found expression of chaperones or oxidative stress enzymes. This was not surprising, since U seemed to cause less direct oxidative damage than metals such as cadmium or chromate (Hu et al., 2005). This might also be explained by the fact that U was unable to enter *S. bentonitica* cells.

After manual annotation (see section 2.7), more transcripts were identified as affected by uranium and potentially involved in its biomineralization. For instance, genes related to processes such as transport, cell wall and lipopolysaccharide biosynthesis, and phosphate metabolism (among others) were up-regulated.

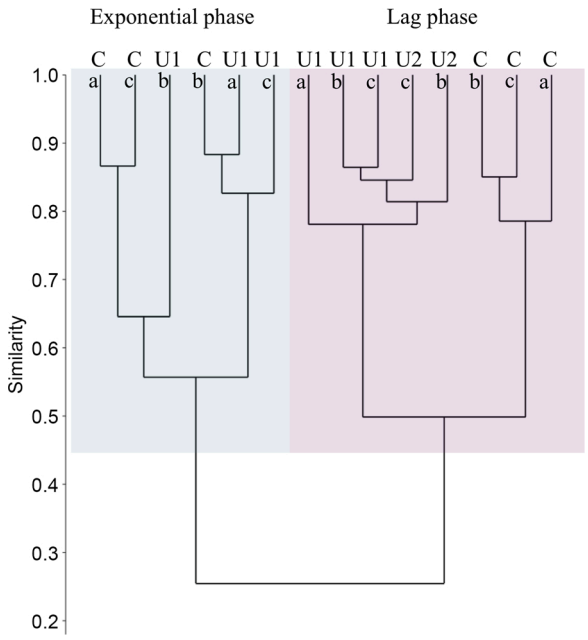

Fig. 5. RNA profiles clustering according to similarity between replicates of each sample (a, b and c). Gene expression during lag phase was clearly different from that in exponential phase. Treated samples also grouped separately from the untreated samples during lag phase.

3.3.1. *Transporters*

Fig. 7 reflects the complex response of the transporters involved in cations, drugs and toxic compound transport —such as resistance-nodulation-cell division (RND transporters) efflux system, ABC transporters (ATP-binding cassette) or the TonB-dependent receptors— that showed different expression levels in U-exposed cell cultures.

Genes pertaining to *RND transporters* were highly expressed in U treated cells, mainly in the early hours of the experiment (lag phase), with fold changes up to 9.8 and 6.7, respectively in 100 μM and 250 μM. Several studies have shown the ability of RND family proteins to prevent the toxicity of various heavy metals. Members of this family associate with membrane proteins or factors to form a protein complex that permits export of the substrate outside the cells. Among these RND transporters, CzcCBA complex was firstly described in *Ralstonia metallidurans* as conferring Co^{2+}, Zn^{2+}, Cd^{2+} and Ni^{2+} resistance (Nies, 2003). Moreover, Orellana et al. (2014) reported a higher abundance of this protein complex in *Geobacter sulfurreducens* proteome in presence of 100 μM of uranyl acetate, highlighting its role in U tolerance. *S. bentonitica* showed up-regulation of two genes encoding for CzcA/CusA and one for CzcD (1.6-, 1.62- and 2.2-fold changes, respectively) in the exponential phase under 100 μM of U. However, none of these genes were detected during the lag phase.

Transcripts encoding SmeE and SmeD were up-regulated (Fig. 7), but the associated protein of the complex, SmeF was not detected. Similar results were observed for AcrA and AcrB, and MdtA, B and C. The function of these systems in antibiotic resistance has been demonstrated (Hayashi et al., 2015; Nies, 2003). Still, no information regarding their involvement in heavy metal tolerance is known.

In accordance with previous studies involving several heavy metals, including U (Yung et al., 2015), genes belonging to ABC transport systems were also positively regulated in this study, mainly during lag phase, varying in a range from 6 to 9-fold changes for 100 μM, and from 5 to 6-fold changes for 250 μM. Among them, the subunit CcmA was up-regulated, which along with CcmB and C, is involved in cytochrome c assembly (Feissner et al., 2006). Nevertheless, no transcripts were found for CcmB nor C. ABC transporters allow for the transport of drugs and toxic compounds across the membrane (Marquez, 2005). Although up-regulation of ABC transporters has been previously observed in presence of U (Choudhary et al., 2012), there is no evidence of this system's implication in U detoxification, and the substrate translocated is still unknown (Verissimo and Daldal, 2014).

Another class of transporters whose expression was modulated under U stress were the TonB-dependent receptors. Different TonB-dependent receptors were up-regulated during the lag phase, especially under 100 μM of U (Fig. 7). It is an outer membrane receptor that interacts with TonB protein to couple the energy needed for high specificity translocation across the outer membrane of different substrates (e.g. iron siderophores or cobalamins) (Chimento et al., 2003). Several studies reported a higher abundance of these transporters in the presence of heavy metals, suggesting an important role in heavy metal resistance (Hu et al., 2005; Yung et al., 2014). Hu et al. (2005) furthermore observed this phenomenon when cells of *C. crescentus* were exposed to U, Cd and Cr, particularly in the latter. But the up-regulation of TonB-dependent protein may be also unrelated to transport processes. The receptor could bind to heavy metals to carry out signaling processes that give environmental information to the cells.

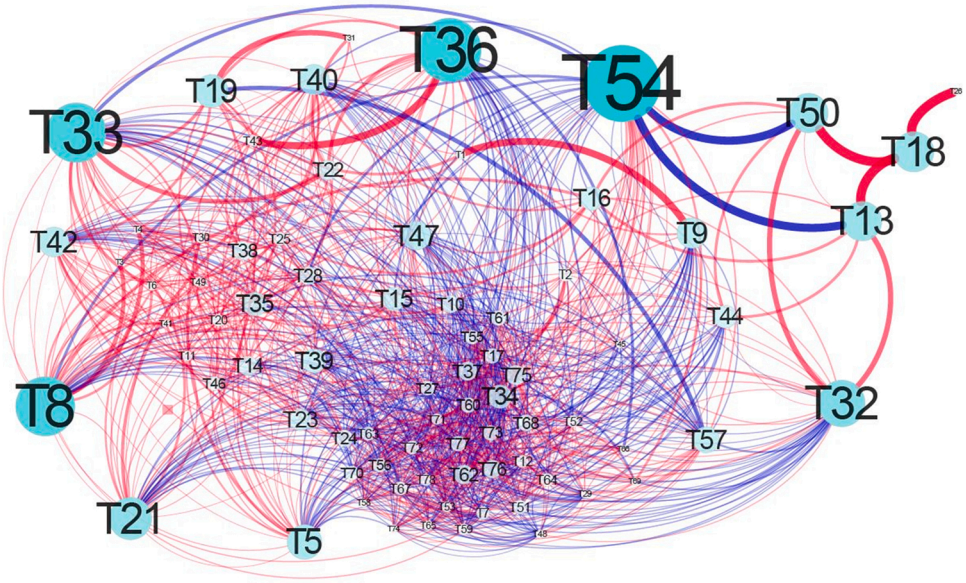

Fig. 6. Interaction network between gene transcripts during time 1. Positive and negative correlations are represented in red and blue lines, respectively. T54 (*ribonucleotide reductase class I)*, T50 (*phoU)*, T13, T18 (*tonB-dependent receptors*), T8 (*RND efflux system*), and T33 (*tail-specific protease*) expression showed interaction with a high number of transcripts at this incubation time. See supplementary table S1 for the complete nomenclature and the Pearson correlation coefficient of each transcript.

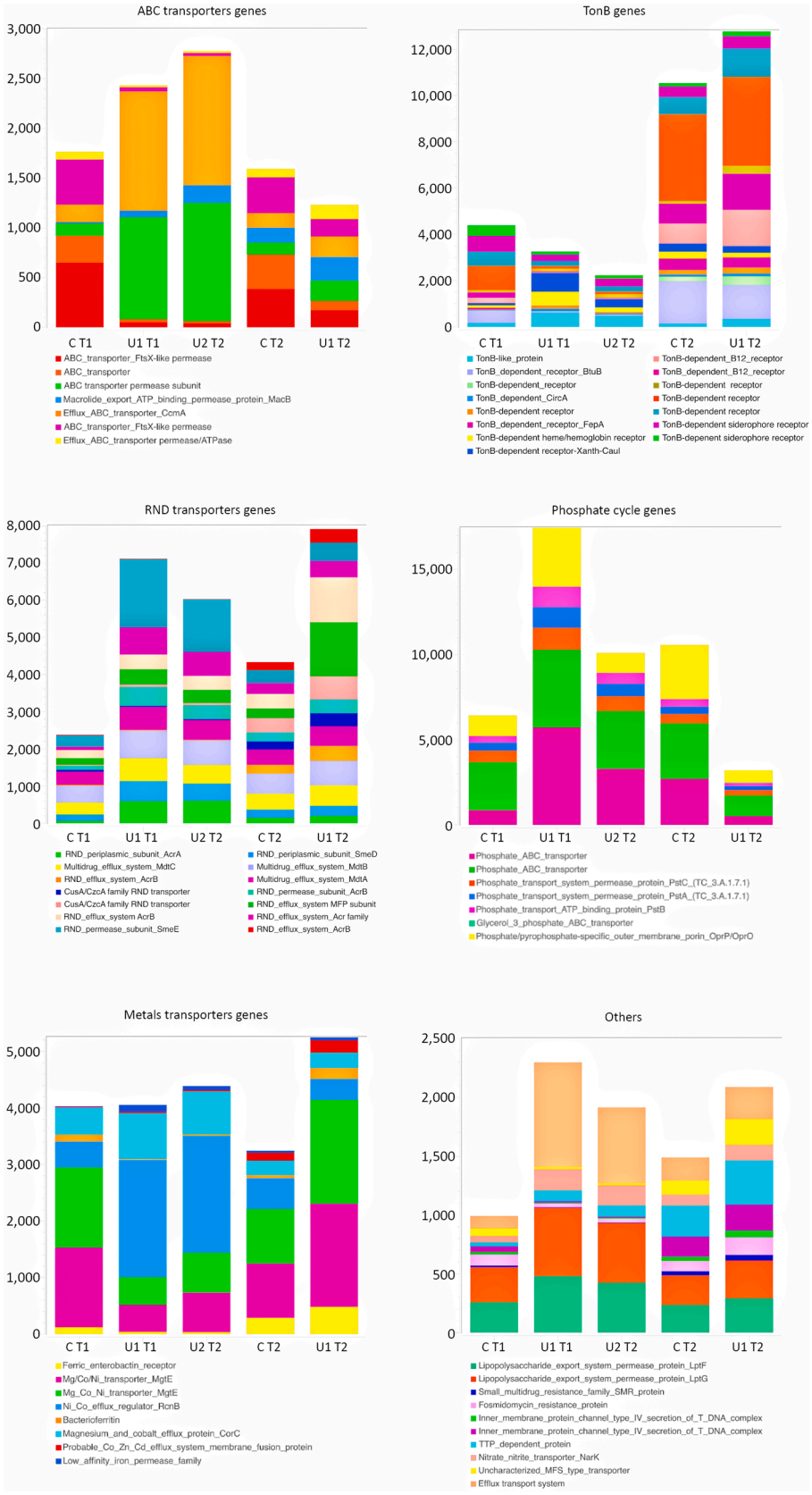

Fig. 7. Distribution of transcripts encoding different transporters in absence (C) and in presence of 100 (U1) and 250 μM (U2) of uranyl nitrate, during the lag (T1) and exponential (T2) phases.

Other transcripts involved in the specific transport of metals were detected. A Ni^{2+}/Co^{2+} efflux regulator RcnB was 4.5-fold up-regulated during the lag phase, but down-regulated in the exponential phase. Furthermore, a $Mg^{2+}/Co^{2+}/Ni^{2+}$ transporter MgtE showed the opposite behavior, being down-regulated in the lag phase, but it was 1.9-fold higher than in the untreated cells during the exponential phase.

While the role of some of these genes in the transport of cations such as Co^{2+}, Zn^{2+} or Na^{2+} to maintain metal homeostasis of the cells has been extensively described (Fath and Kolter, 1993; Nies, 2003), no information exists about the involvement of these systems in U transport. U intracellular accumulation can cause damage to proteins and DNA due to its affinity to thiol or carboxyl groups. Given the lack of any known biological function of this radionuclide, bacteria would have to use transporters that serve to maintain metal cation homeostasis, to export U from the cells (Choudhary et al., 2012; Orellana et al., 2014). The up-regulation of transporters implicated in the efflux of different substrates, i.e. antibiotic export, could be related to other processes triggered by U toxicity such as the envelope stress response. Hence, these genes could play an important structural role associated with the cell envelope stability, as was demonstrated for the SmeIJK system in *S. maltophilia* (Huang et al., 2014).

In contrast with previous results, certain transcripts of transporter proteins—ABC transporters, TonB-dependent receptors, or Mg, Co and Ni transporters— were down-regulated in all sampled metal concentrations and times, probably due to membrane perturbation caused by metal stress (Yung et al., 2014).

It is also worth noting that expression levels of genes implicated in phosphate transport in the untreated cells during lag phase are similar to those obtained for the U-treated cells at time 2, and vice versa. These results could be explained by the effect of U on the cell metabolism. On the one hand, there is no growth during the lag phase of treated samples, but the up-regulation of phosphate transporters suggests the use of phosphate for U removal through its precipitation as U phosphates (Fig. 2A). On the other hand, untreated cells increased P uptake to face the requirements for growth during the exponential phase, whereas this uptake decreased in U-treated cells, as most of the U had already been removed. Furthermore, the treated cells required less P to grow, since the growth rate is lower in these samples, which explains the higher expression of these genes in untreated cells despite being in the same growth phase.

3.3.2. Cell wall and lipopolysaccharide biosynthesis

Exposure to U changed the expression of genes encoding cell wall and membrane proteins, which play a key role in maintaining membrane integrity and in cell envelope synthesis. These changes were dependent on the incubation time and the concentration of the metal, the main changes being observed after 1 h of incubation (lag phase) at 100 μM of U. A high number of transcripts belonging to CreD protein and GTB-type superfamily glycosyltransferase (GT), followed by the proteins OmpA, LolA, an ArnT GT, and a lipid-A disaccharide synthase, were observed in U treated samples after 1 h of incubation (Fig. 8). Some genes involved in biofilm formation, such as *degQ* (Wang et al., 2015), were also up-regulated during the lag phase (4.5- and 3.4-fold change under 100 and 250 μM, respectively).

It is noteworthy that *creD* encoding an inner membrane protein was highly induced (21-fold) in the presence of 250 μM of U. Huang et al. (2015) investigated the possible functions of CreD in *S. maltophilia*. Mutants lacking this protein showed altered outer membrane permeability, suggesting it is key for cell envelope homeostasis and integrity. They also proved that CreD protein increased in the case of high bacterial density, probably to address inner membrane expansion. As up-regulation of CreD in *S. bentonitica* was observed during the lag phase, this supports a possible key role in U tolerance by decreasing the permeability of the cell envelope, preventing the metal from reaching the cytoplasm.

Furthermore, genes also located in the *cre* locus (Fig. S4) have been

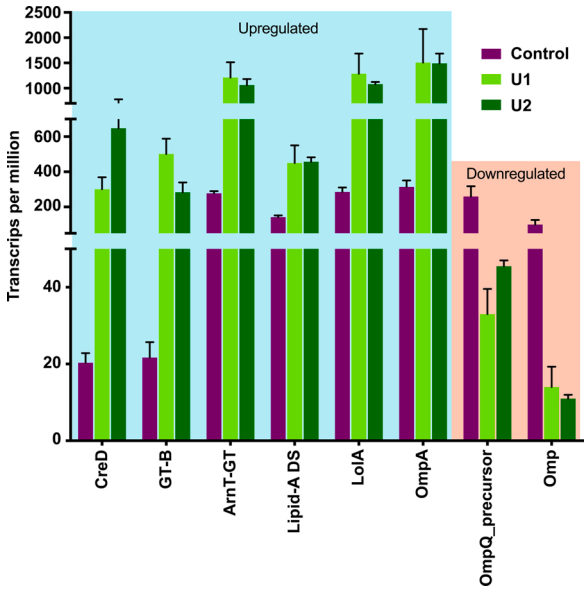

Fig. 8. Genes encoding membrane proteins, enzymes and proteins taking part in cell wall structure biosynthesis that changed their expression under U exposure during lag phase. Expression levels are shown as transcript per million (tpm).

previously related to the phosphate metabolism. In P_i starvation conditions, *creC* can act as a response regulator of the CreBC two-component system involved in phosphorylation of PhoR, required for the expression of the alkaline phosphatase PhoA (Cariss et al., 2008). It has been demonstrated that CreBC strongly induces *creD* expression in *E. coli* DH5α (Avison et al., 2001). Notwithstanding, Huang et al. (2015) showed that CreBC regulated negatively the activity of *creD*.

Up-regulation levels of 23- and 4-fold, respectively, of a glycosyltransferase B superfamily (GT-B) and ArnT belonging to the GT-C superfamily were observed in 100 μM, and to a lesser extent under 250 μM of U treatment (13- and 2.5-fold). Another type of GT from family 19, the Lipid A disaccharide synthase (LpxB), was found 3-fold higher after 1 h of 100 μM of U exposure, as compared to untreated cells. Bacterial GT consists of inner membrane enzymes known to be involved in several biosynthetic processes. Up-regulated GT participates in lipopolysaccharide (LPS) biosynthesis by adding sugar residues at different levels to the LPS structure. The GTB-type is closely related to the GT1 family, whose members take part in LPS biosynthesis by adding activated nucleotide sugar to the core oligosaccharide (Luke et al., 2010; Schmid et al., 2016). In turn, ArnT is characterized by the addition of 4-amino-4-*deoxy*-L-arabinose (L-Ara4N) residues to the lipid A of LPS (Tavares-Carreón et al., 2015). LpxB, located in the cytoplasmic membrane, takes part in the synthesis of the intermediary molecule lipid A disaccharide, a precursor necessary for the lipid A formation of LPS (Metzger and Raetz, 2009).

The LPS of Gram-negative bacteria is known to protect the cells from antimicrobial compounds by avoiding their diffusion, and GT activity could lead to modifications in the oligosaccharide structure that provides resistance to these compounds, as occurs with the addition of L-Ara4N residues to lipid A of LPS, and polymixin resistance (Rosenfeld and Shai, 2006; Tavares-Carreón et al., 2015). Therefore, it can be surmised that the up-regulation of these GT enzymes would physically block U entrance. The L-Ara4N modifications observed could also result in changes in the global structure of the LPS to promote a more specific response to the presence of the metal. The two processes might act together to conform an efficient mechanism for U tolerance.

A periplasmic protein encoded by the gene *lolA* was also up-regulated at both U concentrations tested after 1 h of incubation (5-fold and 2.5-fold under 100 and 250 μM, respectively). LolA is a

chaperone belonging to the Lol system, which comprises five proteins: LolA, B, C, D and E. The proteins LolCDE of this system form an inner membrane ABC transporter, which interacts with the periplasmic protein LolA to transfer lipoproteins such as Pal. Then, LolA associates with LolB in order to anchor the lipoprotein at the outer membrane (Murahari et al., 2013). Similar results were found for *G. sulfurreducens*, whose proteome in presence of U likewise showed an up-regulation of LolB, as well as other outer membrane lipoproteins (Orellana et al., 2014). The slight up-regulation of the rest of the Lol complex (B, C, D and E) indicates that the cells were actively involved in biogenesis of the outer membrane under U stress.

Up-regulation of *ompA* was observed when *S. bentonitica* grew with 100 and 250 μM of U (5- and 3-fold changes, respectively). OmpA is a two-domain outer membrane porin highly expressed in Gram-negative bacteria and tightly regulated by environmental changes (Smith et al., 2007). This protein has been linked to cell survival under environmental stress, and the maintenance of cell shape and membrane integrity (Sonntag et al., 1978; Wang, 2002). The fact that a TonB-dependent receptor related to OmpA was down-regulated under 250 μM of U could be explained by the higher toxicity under this concentration. The up-regulation of this protein suggests that an increase of the surface of the outer membrane may occur, hindering intracellular U accumulation by BII-R7 cells (Nilsson et al., 1984). Because such a response has been described with other heavy metals like Cr in *C. crescentus* (Hu et al., 2005), it might be a general response to various heavy metal stresses.

In contrast to OmpA, the expression of a phosphate-selective porin belonging to the Phosphate-selective porin O/P family, *oprP*, decreased when cells reached the middle-exponential phase (52 h) under 100 μM of U. This outer membrane protein exhibits a high affinity for polyphosphate anions (Modi et al., 2015). Dekker et al. (2016) obtained similar results with a porin of the same family, Omp40, when *A. ferrooxidans* were exposed to 0.5 mM of U(VI). These authors suggested that the protein's down-regulation could be a means of impeding the passage of the radionuclide-phosphate complex through the membrane, given the affinity of phosphate ions to the metal.

The results of our study suggest that U exposure could have an effect on the σ^E regulon. Up-regulation of RNA polymerase σ factors E (*rpoE*) was also observed after 1 h, especially under 100 μM of U. Envelope stress caused by metal sorption to the surface activates σ^E, which explains the up-regulation of genes involved in the rearrangement of LPS and membrane composition (Mitchell and Silhavy, 2019). However, σ^E also triggers the synthesis of *micA*, a small RNA that inhibits the expression of *ompA* (Brooks and Buchanan, 2008; Smith et al., 2007). The up-regulation of *ompA* observed is therefore explained by the presence of the inner membrane protein RseA (3.45- and 2.32-fold change under 100 and 250 μM, respectively) that represses σ^E function (Mitchell and Silhavy, 2019).

The cell wall is the first barrier that bacteria can use to protect themselves from toxic compounds, including heavy metals. Indeed, microbial biomass shows high affinity to U. Metal cation complexation on the surface of bacteria has also been widely described in the context of biosorption.

Since a bacterial surface has a number of charged functional groups within its layers, it makes direct contact with the environment and affords centers for metal cation binding by means of electrostatic and Van der Waals interactions with carboxyl, phosphate, hydroxyl and amine groups. The presence of a metal could affect the distribution of these ligands, increasing cell wall and LPS structures, and explaining the up-regulation of these genes in *S. bentonitica* (Merroun and Selenska-Pobell, 2008; Zhang et al., 2018). This is known as the fast metabolism-independent mechanism. It occurs during the first minutes of metal exposure (Celik et al., 2018; Yang et al., 2015), and has been described for many other bacteria when in contact with U. According to Gerber et al. (2016), this chelation process takes place in *Acidovorax facilis* within the first 8 h of incubation with U at pH 5, followed by a slower process of U accumulation in the cytoplasm; fast U adsorption was also observed in *Microbacterium oleivorans* A9 incubated at different temperatures and concentrations of the metal (Theodorakopoulos et al., 2015).

Several studies depict the bacterial surface as a dynamic structure able to vary even in a single cell in response to the surrounding environment, determining the distribution of ligands and proteins within it (Khalid et al., 2008). A presence of heavy metals in the growing medium could give rise to an overexpression of genes related to cell wall and lipopolysaccharide synthesis, thus explaining the gene up-regulation seen for *S. bentonitica* in our study (Merroun and Selenska-Pobell, 2008; Zhang et al., 2018).

3.3.3. Phosphate metabolism and U biomineralization

The transcriptomic analyses performed detected an up-regulation of phosphatase in U treated cells after 1 h of incubation (lag phase), suggesting how important this type of enzyme may be for coping with metal stress. Despite the fact that 43 genes encoding phosphatases were detected, only four of them showed high induction when cells of BII-R7 were exposed to both 100 and 250 μM of U. Remarkably, one acid and one alkaline phosphatase were found about 7-fold higher than in the untreated cells under 100 μM of U in lag phase (Fig. 9). This finding suggests that U enhanced the native phosphatase activity, supported by the increase in P_i observed in the supernatant (Fig. 2B). In addition, the wide range of phosphatases identified in *S. bentonitica* cells could condition its adaptation to the low-P environment of bentonite formations where this strain was isolated, through a variety of organic P sources (Skouri-Panet et al., 2018).

Within the sampling time 2 (52 h), four types of phosphatase showed significant changes in their expression levels. Alkaline and acid phosphatases were also up-regulated, yet to a lesser extent than after 1 h of incubation. The other two proteins —an inositol-1-monophosphatase and inorganic pyrophosphatase— were down-regulated when cells were exposed to U. Bacterial phosphatases, both acid and alkaline, are assumed to play a major role in U biomineralization, leading to the formation of U-phosphate mineral phases when using organic phosphate as P_i source, reducing U availability and toxicity in the environment (Chandwadkar et al., 2018).

The alkaline phosphatase up-regulated in *S. bentonitica* BII-R7 is related to an inner membrane phosphoethanolamine transferase (with 100% similarity) similar to OpgE from *E. coli* (E-value 6.05e-99). This enzyme catalyzes the substitution of constitutive glucose from osmoregulated periplasmic glucans (OPGs) by phosphoethanolamine residues (Bontemps-Gallo et al., 2013). Modifications of OPGs with phosphoglycerol, succinyl and/or phosphoethanolamine confer an anionic character to the molecule (Bontemps-Gallo et al., 2017). Thus, the addition of phosphoethanolamine to OPGs could promote the biosorption process previously mentioned by providing U binding sites (see section 3.3.2).

Further studies have highlighted the importance of diverse alkaline phosphatases in U(VI) biomineralization. Yung and Jiao (2014) proposed a U(VI)-biomineralization mechanism in *C. crecentus* NA1000 mediated by the naturally-expressed periplasmic PhoY. This non-specific ALP-like superfamily phosphatase produced extracellular precipitates of meta-autunite $[(NH_4)(UO_2)(PO_4)\cdot 3H_2O]$ —the uranyl phosphate species of U(VI)— by releasing P_i to the medium from G2P. Similar results are described for PhoK from *Sphingomonas* sp. BSAR-1 when up-regulated in *E. coli* and *D. radiodurans* (Kulkarni et al., 2013; Nilgiriwala et al., 2008). Thus, this enzyme may enhance U resistance via two processes: biosorption of U to the surface through increasing LPS production; and additional promotion of the biomineralization process once U is linked to the membrane.

The acid phosphatase found in the present study belongs to the membrane-associated type 2 phosphatidic acid phosphatase (PAP2) superfamily. Appukuttan et al. (2011) investigated the role of *phoN* —a periplasmic nonspecific acid phosphatase also included in the PAP2 superfamily— in U biomineralization by means of a *phoN*-expressing *D. radiodurans* strain; they showed that lyophilized cells could achieve 100% precipitation in the presence of 10 mM of uranyl nitrate after 13

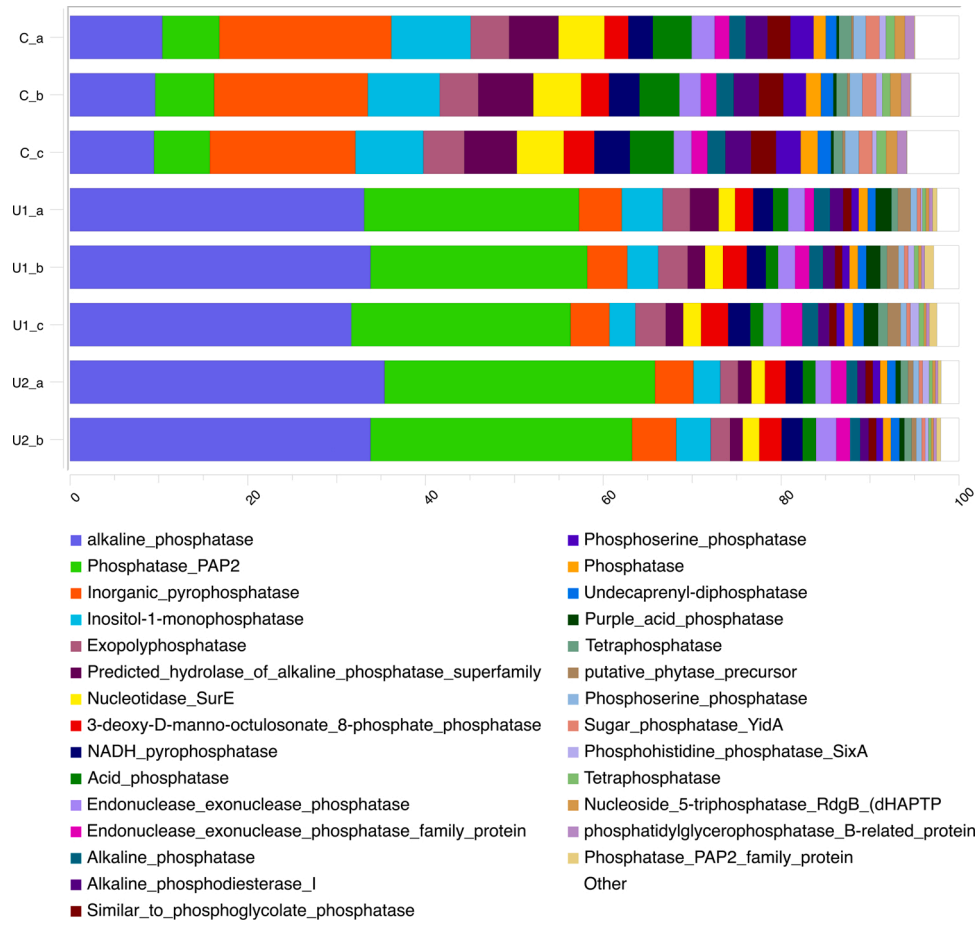

Fig. 9. Differential expression of genes with phosphatase activity in *S. bentonitica*, in presence (U1, U2) and absence (C) of uranium. Transcripts shown correspond to lag phase (1 h of incubation).

days, whereas complete depletion of higher concentrations of U (15 and 20 mM) was reached after 17 days. Scanning Electron Microscopy revealed that the precipitated U was mainly associated with the cell membranes, without signs of extracellular precipitation. In the study by Xu et al. (2018), the same recombinant bacterium, when exposed to 1 mM of uranyl acetate, was able to precipitate up to 95% of uranium after 13 h.

In light of the microscopic results obtained in this study (see section 3.2), the interaction of U with the cells of BII-R7 signals a biphasic process. At first, a fast process mediated by biosorption of U to the cell surface through phosphate-containing molecules (including proteins) is enhanced by the up-regulation of membrane proteins described above. This rapid process lays out a nucleation site for precipitation of the metal (Merroun and Selenska-Pobell, 2008), which is conditioned by phosphatase activity in the second phase. The U-phosphate minerals formed would be released from the cells to the extracellular medium. Several studies evoke this two-phase precipitation model as a very likely phenomenon in bacteria possessing the ability to precipitate U (Chandwadkar et al., 2018; Liang et al., 2016).

Furthermore, the cellular location of U phosphates apparently depends mostly on the aqueous U species predominant under specific conditions, rather than on the enzyme location. Kulkarni et al. (2016) investigated U precipitation in terms of acid (*phoN*) and alkaline (*phoK)* phosphatases, expressing the enzymes from *Salmonella enterica* serovar Typhimurium in *E. coli* and *D. radiodurans*. They affirmed that carbonate-deficient conditions triggered mainly cell-bound bioprecipitation, while carbonate-abundant conditions led to an extracellular location of precipitates; phosphatase activity yielded chernikovite $[H_2(UO_2)_2(PO_4)_2{\cdot}8H_2O]$ at pH 6.8. Differential locations of U precipitates were also described for *Serratia* sp. strain OT II 7 cells after incubation at pH 5, 7 and 9 (Chandwadkar et al., 2018). Neutral and alkaline conditions resulted in the precipitation of calcium uranyl phosphate hydrate $[Ca(UO_2)_2(PO_4)_2{\cdot}6H2O]$, mainly distributed in the extracellular medium. However, at pH 5, uranyl phosphate hydrate $[HPUO_6{\cdot}4H_2O]$ as well as calcium uranyl phosphate hydrate were observed, mostly as intracellular accumulations. These results suggest that the location of U precipitates is determined by the pH of the culture medium, which in turn conditioned the metal speciation, the type of phosphatase enzyme (acid or alkaline) exhibiting more activity, and the binding capacity of the functional groups of the cell wall.

A 3-fold induced polyphosphate kinase (*ppk*) was detected in presence of 100 μM after 1 h of incubation. The immobilization of U and other metals in polyphosphate granules —a mechanism conferring tolerance— has been widely reported (Acharya and Apte, 2013; Hu et al., 2005; Sivaswamy et al., 2011). In a study by Suzuki and Banfield (2004), *Arthrobacter ilicis* increased the amount of polyphosphate granules when it was exposed to U, pointing to a significant role of polyphosphates in the immobilization of uranyl ions to avoid cellular damage. EDX analysis of the polyphosphates generated by BII-R7 revealed, however, that U did not accumulate in these granules (data not shown). The expression of this enzyme might therefore be induced in response to the presence of G2P in the culture medium, stored as a source of P by synthesizing polyphosphates to be later used for U precipitation (Gallois et al., 2018). An absence of *ppk* expression during the exponential growth phase may owe to depletion of P_i used earlier in U biomineralization.

In this study, transcripts of genes involved in specific P uptake and metabolism (such as pho regulon genes) were also identified. Expression of genes of the *pstSCAB* system, *phoB* and *phoU*, changed especially after 1 h of incubation (lag phase). PhoB and PhoU are transcriptional

regulators that respectively control, positively and negatively, the transcription of phosphate regulon genes. PhoB accumulation has been linked to phosphate starvation conditions, activating transcription of *pstSCAB* to allow the high-affinity import of P_i inside the cell (Chen et al., 2015; Santos-Beneit, 2015). Given the G2P-rich conditions in the culture medium, in this study *phoU* exhibited 4-fold induction in the presence of 100 μM of U. The *phoB* (1.86-fold change) and *pst* system (1.9-, 2.57- and 3.11-fold changes respectively for PstC, A, and B) were also up-regulated, albeit to a lesser extent.

These findings suggest that both PstSCAB and PhoB may increase during the first minutes of incubation in order to transcribe the phosphatases that release P_i from G2P. Part of the released P_i could be used not only to address cellular requirements, but also to synthesize polyphosphate granules via PPK activity (as described above); then, PhoU would intervene to stop P_i import, thereby impeding the possibly toxic effects of an excess of this compound (Santos-Beneit, 2015). The demonstrated lack of these processes at concentration 250 μM and in the middle-exponential growth phase could be attributed, respectively, to the toxic effects of the metal and the adaptation of the cells to the conditions of exposure. Meanwhile, part of P_i would have interacted with uranyl to form uranyl-phosphate minerals.

3.3.4. Iron transport and metabolism

Some previous studies related U exposure to an increase in proteins governing iron uptake and metabolism (Gallois et al., 2018; Orellana et al., 2014). Analysis of the expression regulation of genes involved in iron metabolism in our samples was therefore deemed necessary. Three ferrichrome-iron receptors located in the outer membrane (involved in the import of Fe^{3+}-siderophore complexes into the periplasmic space) were detected in the samples treated with 100 μM U for 1 h. The most abundant one, with 2.3-fold change, shared similarity with the Fiu domain sequence; the other two belonged to CirA superfamily receptors, which exhibited changes 2.27- and 1.75-fold higher than in control samples.

Fiu and CirA proteins are outer membrane transporters that import Fe^{3+} attached to catecholate siderophores by interacting with TonB and inner membrane proteins. These interactions provide energy for transport (Andrews et al., 2003; Grinter and Lithgow, 2019). Once inside the cell, proteins such as bacterioferritin-associated ferredoxin (up-regulated 1.85-fold) can reduce Fe^{3+}, then release it from the ferrichrome under iron restriction conditions. Furthermore, a gene belonging to a *feoB* superfamily protein was slightly up-regulated in our study (1.43-fold change). The function of this protein, located in the cytoplasmic membrane, is Fe^{2+} uptake, usually under anaerobic conditions, where the stability of this ion is higher (Andrews et al., 2003).

Transcripts of genes encoding the cytosolic proteins NufA and SufB were also found in higher proportions only at 1 h of 100 μM of uranyl exposure, with fold changes ranging between 1.62 and 1.66. These genes are induced under oxidative stress to help form [Fe-S] clusters and act as chaperones to repair damaged [Fe-S] proteins as well. SufB is part of the SufABC complex, which is regulated by the Fur protein, which controls the transcription of many genes, including those involved in divalent metal ion uptake (Andrews et al., 2003; Troxell and Hassan, 2013). In presence of Fe^{2+}, the Fur-Fe^{2+} complex binds to DNA to prevent transcription of Fe^{3+}, and the same process has been observed for Mg^{2+} or Co^{2+}. According to the results obtained here, *fur* gene was down-regulated (-1.26- and -1.98-fold changes under 100 and 250 μM, respectively). Orellana et al. (2014) reported, in contrast, that Fur protein was more abundant under U exposure in *G. Sulfurreducens*.

Although these genes were not detected at 52 h of incubation, a ferric enterobactin receptor was up-regulated (1.68-fold) through the same mechanism as described for Fiu and CirA to obtain the enterobactin siderophore.

Gallois et al. (2018) expounded an induction of proteins involved in the iron metabolism of the proteome of *M. oleivorans* A9 strain when exposed to 10 μM of uranyl nitrate at pH 5. This bacteria demonstrated its ability to form intracellular U(VI)-phosphate accumulations when exposed to 50 μM of uranyl nitrate; U tended to be uptaken via proteins involved in the iron transport (Gallois et al., 2018). As some siderophores showed high affinity to U, the above authors proposed that iron uptake systems could influence the intracellular accumulation of U, as put forth in studies demonstrating the ability of this strain to form intracellular accumulations containing U (Theodorakopoulos et al., 2015). The microscopic analyses undertaken here showed that BII-R7 is not able to bioaccumulate U, yet the variation in the location of the minerals could be due to the influence of the pH, as previously suggested in this study. Still, all the mentioned genes were induced under iron-starvation conditions. Their slight up-regulation might be explained by the lack of Fe sources in the used culture medium, but also as an indirect effect of U exposure. The increase in the P_i induced by the metal would lead to the formation of Fe-P complexes, thereby reducing the availability of Fe for the cells.

4. Conclusions

This study describes the response of the novel bacterial strain *Stenotrophomonas bentonitica* BII-R7 in the presence of U. U removal experiments demonstrate its effectiveness in eliminating 97% of the U present in the medium after 24 h of incubation at 100 μM of U; and 96% when exposed to 250 μM. Analysis of gene expression during U exposure revealed a high up-regulation of genes involved in cell wall biosynthesis, transport of toxic compounds, and acid and alkaline phosphatases. Cell wall proteins such as CreD and OmpA —crucial for maintaining membrane integrity— may block the entrance of U inside the cells when up-regulated. According to microscopic observations, soluble uranyl ions would bind to functional groups of the cell wall of *S. bentonitica*, where they precipitate to form U-phosphate minerals due to the phosphatase activity of PAP2 or ALP-like phosphatases. Meanwhile, transport systems (e.g. RND transporters) would prevent U accumulation inside the cells by means of active efflux of the metal. Altogether, the results of this work provide quality information about the behaviour of this bacterium at the molecular level, which is of high relevance for understanding how bacteria cope with radionuclides, and for designing effective bioremediation strategies.

CRediT authorship contribution statement

Pinel-Cabello M.: Methodology, Investigation, Formal analysis, Writing - original draft. **Jroundi F.:** Conceptualization, Supervision, Methodology, Investigation, Writing - original draft. **López-Fernández M.:** Investigation. **Geffers R.:** Resources. **Jarek M.:** Resources. **Jauregui R.:** Resources. **Link A.:** Resources. **Vílchez-Vargas R.:** Conceptualization, Supervision, Methodology, Formal analysis, Resources, Writing - original draft. **Merroun M.L.:** Conceptualization, Supervision, Methodology, Resources, Writing - original draft.

Declaration of Competing Interest

The authors report no declarations of interest.

Acknowledgements

This work was supported by the grants FPU 15/04284 ("Formación de Profesorado Universitario") and EST 17/00739 ("Ayudas a la movilidad para estancias breves y traslados temporales") obtained by the first author, from the Spanish Ministry (Ministerio de Educación, Cultura y Deporte), and from the European projects MIND-661880 and CGL2014-59616-R. Alexander Link and Ramiro Vílchez-Vargas are supported by the grants from the European Regional Development Fund of the European Commission. The authors are grateful to Concepción Hernández-Castillo and María del Mar Abad Ortega for their assistance at Microscopy services (*Centro de Instrumentación Científica*, University of Granada), to Maren Scharfe for technical support at sequencing services

(Genome Analytics, Helmholtz Centre for Infectious Diseases) and to Jean Sanders for English revision of the manuscript.

Appendix A. Supplementary data

Supplementary material related to this article can be found, in the online version, at doi:https://doi.org/10.1016/j.jhazmat.2020.123858.

References

Acharya, C., Apte, S.K., 2013. Novel surface associated polyphosphate bodies sequester uranium in the filamentous, marine cyanobacterium, *Anabaena torulosa*. Metallomics 5, 1595. https://doi.org/10.1039/c3mt00139c.

Andrews, S.C., Robinson, A.K., Rodríguez-Quiñones, F., 2003. Bacterial iron homeostasis. FEMS Microbiol Rev 27, 215–237. https://doi.org/10.1016/S0168-6445(03)00055-X.

Appukuttan, D., Seetharam, C., Padma, N., Rao, A.S., Apte, S.K., 2011. PhoN-expressing, lyophilized, recombinant *Deinococcus radiodurans* cells for uranium bioprecipitation. Journal of Biotechnology 154, 285–290. https://doi.org/10.1016/j.jbiotec.2011.05.002.

Avison, M.B., Horton, R.E., Walsh, T.R., Bennett, P.M., 2001. *Escherichia coli* CreBC Is a Global Regulator of Gene Expression That Responds to Growth in Minimal Media. J. Biol. Chem. 276, 26955–26961. https://doi.org/10.1074/jbc.M011186200.

Bader, M., Rossberg, A., Steudtner, R., Drobot, B., Großmann, K., Schmidt, M., Musat, N., Stumpf, T., Ikeda-Ohno, A., Cherkouk, A., 2018. Impact of Haloarchaea on Speciation of Uranium—A Multispectroscopic Approach. Environ. Sci. Technol. 52, 12895–12904. https://doi.org/10.1021/acs.est.8b02667.

Beazley, M.J., Martinez, R.J., Sobecky, P.A., Webb, S.M., Taillefert, M., 2009. Nonreductive Biomineralization of Uranium(VI) Phosphate Via Microbial Phosphatase Activity in Anaerobic Conditions. Geomicrobiology Journal 26, 431–441. https://doi.org/10.1080/01490450903060780.

Beazley, M.J., Martinez, R.J., Sobecky, P.A., Webb, S.M., Taillefert, M., 2007. Uranium Biomineralization as a Result of Bacterial Phosphatase Activity: Insights from Bacterial Isolates from a Contaminated Subsurface. Environ. Sci. Technol. 41, 5701–5707. https://doi.org/10.1021/es070567g.

Bone, S.E., Dynes, J.J., Cliff, J., Bargar, J.R., 2017. Uranium(IV) adsorption by natural organic matter in anoxic sediments. Proc Natl Acad Sci USA 114, 711–716. https://doi.org/10.1073/pnas.1611918114.

Bontemps-Gallo, S., Bohin, J.-P., Lacroix, J.-M., 2017. Osmoregulated Periplasmic Glucans. EcoSal Plus 7. https://doi.org/10.1128/ecosalplus.ESP-0001-2017.

Bontemps-Gallo, S., Cogez, V., Robbe-Masselot, C., Quintard, K., Dondeyne, J., Madec, E., Lacroix, J.-M., 2013. Biosynthesis of Osmoregulated Periplasmic Glucans in Escherichia coli: The Phosphoethanolamine Transferase Is Encoded by opgE. BioMed Research International. https://doi.org/10.1155/2013/371429.

Boyanov, M.I., Fletcher, K.E., Kwon, M.J., Rui, X., O'Loughlin, E.J., Löffler, F.E., Kemner, K.M., 2011. Solution and Microbial Controls on the Formation of Reduced U (IV) Species. Environ. Sci. Technol. 45, 8336–8344. https://doi.org/10.1021/es2014049.

Brooks, B.E., Buchanan, S.K., 2008. Signaling mechanisms for activation of extracytoplasmic function (ECF) sigma factors. Biochimica et Biophysica Acta (BBA) - Biomembranes 1778, 1930–1945. https://doi.org/10.1016/j.bbamem.2007.06.005.

Cariss, S.J.L., Tayler, A.E., Avison, M.B., 2008. Defining the Growth Conditions and Promoter-Proximal DNA Sequences Required for Activation of Gene Expression by CreBC in *Escherichia coli*. Journal of Bacteriology 190, 3930–3939. https://doi.org/10.1128/JB.00108-08.

Celik, F., Camas, M., Kyeremeh, K., Sazak Camas, A., 2018. Microbial Sorption of Uranium Using *Amycolatopsis* sp. K47 Isolated from Uranium Deposits. Water, Air, & Soil Pollution 229. https://doi.org/10.1007/s11270-018-3766-5.

Chandwadkar, P., Misra, H.S., Acharya, C., 2018. Uranium biomineralization induced by a metal tolerant *Serratia* strain under acid, alkaline and irradiated conditions. Metallomics 10, 1078–1088. https://doi.org/10.1039/C8MT00061A.

Chen, L., Hu, M., Huang, L., Hua, Z., Kuang, J., Li, S., Shu, W., 2015. Comparative metagenomic and metatranscriptomic analyses of microbial communities in acid mine drainage. The ISME Journal 9, 1579–1592. https://doi.org/10.1038/ismej.2014.245.

Chimento, D.P., Kadner, R.J., Wiener, M.C., 2003. The *Escherichia coli* outer membrane cobalamin transporter BtuB: structural analysis of calcium and substrate binding, and identification of orthologous transporters by sequence/structure conservation. J. Mol. Biol. 332, 999–1014.

Choudhary, S., Islam, E., Kazy, S.K., Sar, P., 2012. Uranium and other heavy metal resistance and accumulation in bacteria isolated from uranium mine wastes. Journal of Environmental Science and Health, Part A 47, 622–637. https://doi.org/10.1080/10934529.2012.650584.

Choudhary, S., Sar, P., 2011. Uranium biomineralization by a metal resistant Pseudomonas aeruginosa strain isolated from contaminated mine waste. Journal of Hazardous Materials 186, 336–343. https://doi.org/10.1016/j.jhazmat.2010.11.004.

Dekker, L., Arsène-Ploetze, F., Santini, J.M., 2016. Comparative proteomics of *Acidithiobacillus ferrooxidans* grown in the presence and absence of uranium. Research in Microbiology 167, 234–239. https://doi.org/10.1016/j.resmic.2016.01.007.

Fath, M.J., Kolter, R., 1993. ABC transporters: bacterial exporters. Microbiol Rev 57, 995–1017.

Feissner, R.E., Richard-Fogal, C.L., Frawley, E.R., Kranz, R.G., 2006. ABC transporter-mediated release of a haem chaperone allows cytochrome c biogenesis. Molecular Microbiology 61, 219–231. https://doi.org/10.1111/j.1365-2958.2006.05221.x.

Fomina, M., Charnock, J.M., Hillier, S., Alvarez, R., Gadd, G.M., 2007. Fungal transformations of uranium oxides. Environmental Microbiology 9, 1696–1710. https://doi.org/10.1111/j.1462-2920.2007.01288.x.

Fredrickson, J.K., Zachara, J.M., Kennedy, D.W., Duff, M.C., Gorby, Y.A., Li, S.W., Krupka, K.M., 2000. Reduction of U(VI) in goethite (α-FeOOH) suspensions by a dissimilatory metal-reducing bacterium. Geochimica et Cosmochimica Acta 64, 3085–3098. https://doi.org/10.1016/S0016-7037(00)00397-5.

Gallois, N., Alpha-Bazin, B., Ortet, P., Barakat, M., Piette, L., Long, J., Berthomieu, C., Armengaud, J., Chapon, V., 2018. Proteogenomic insights into uranium tolerance of a Chernobyl's *Microbacterium* bacterial isolate. Journal of Proteomics 177, 148–157. https://doi.org/10.1016/j.jprot.2017.11.021.

Gavrilescu, M., Pavel, L.V., Cretescu, I., 2009. Characterization and remediation of soils contaminated with uranium. Journal of Hazardous Materials 163, 475–510. https://doi.org/10.1016/j.jhazmat.2008.07.103.

Gerber, U., Zirnstein, I., Krawczyk-Bärsch, E., Lünsdorf, H., Arnold, T., Merroun, M.L., 2016. Combined use of flow cytometry and microscopy to study the interactions between the gram-negative betaproteobacterium *Acidovorax facilis* and uranium(VI). Journal of Hazardous Materials 317, 127–134. https://doi.org/10.1016/j.jhazmat.2016.05.062.

Grinter, R., Lithgow, T., 2019. The structure of the bacterial iron–catecholate transporter Fiu suggests that it imports substrates via a two-step mechanism. J. Biol. Chem. 294, 19523–19534. https://doi.org/10.1074/jbc.RA119.011018.

Hayashi, K., Nakashima, R., Sakurai, K., Kitagawa, K., Yamasaki, S., Nishino, K., Yamaguchi, A., 2015. AcrB-AcrA Fusion Proteins That Act as Multidrug Efflux Transporters. J Bacteriol 198, 332–342. https://doi.org/10.1128/JB.00587-15.

Holmes, D.E., O'Neil, R.A., Chavan, M.A., N'Guessan, L.A., Vrionis, H.A., Perpetua, L.A., Larrahondo, M.J., DiDonato, R., Liu, A., Lovley, D.R., 2009. Transcriptome of *Geobacter uraniireducens* growing in uranium-contaminated subsurface sediments. ISME J 3, 216–230. https://doi.org/10.1038/ismej.2008.89.

Hu, P., Brodie, E.L., Suzuki, Y., McAdams, H.H., Andersen, G.L., 2005. Whole-Genome Transcriptional Analysis of Heavy Metal Stresses in *Caulobacter crescentus*. Journal of Bacteriology 187, 8437–8449. https://doi.org/10.1128/JB.187.24.8437-8449.2005.

Huang, H.-H., Lin, Y.-T., Chen, W.-C., Huang, Y.-W., Chen, S.-J., Yang, T.-C., 2015. Expression and Functions of CreD, an Inner Membrane Protein in *Stenotrophomonas maltophilia*. PLOS ONE 10, e0145009. https://doi.org/10.1371/journal.pone.0145009.

Huang, Y.-W., Liou, R.-S., Lin, Y.-T., Huang, H.-H., Yang, T.-C., 2014. A Linkage between SmeIJK Efflux Pump, Cell Envelope Integrity, and σE-Mediated Envelope Stress Response in *Stenotrophomonas maltophilia*. PLoS ONE 9, e111784. https://doi.org/10.1371/journal.pone.0111784.

Islam, E., Sar, P., 2016. Diversity, metal resistance and uranium sequestration abilities of bacteria from uranium ore deposit in deep earth stratum. Ecotoxicology and Environmental Safety 127, 12–21. https://doi.org/10.1016/j.ecoenv.2016.01.001.

Jauberty, L., Drogat, N., Decossas, J.-L., Delpech, V., Gloaguen, V., Sol, V., 2013. Optimization of the arsenazo-III method for the determination of uranium in water and plant samples. Talanta 115, 751–754. https://doi.org/10.1016/j.talanta.2013.06.046.

Khalid, S., Bond, P.J., Carpenter, T., Sansom, M.S.P., 2008. OmpA: Gating and dynamics via molecular dynamics simulations. Biochimica et Biophysica Acta (BBA) - Biomembranes 1778, 1871–1880. https://doi.org/10.1016/j.bbamem.2007.05.024.

Kulkarni, S., Ballal, A., Apte, S.K., 2013. Bioprecipitation of uranium from alkaline waste solutions using recombinant Deinococcus radiodurans. Journal of Hazardous Materials 262, 853–861. https://doi.org/10.1016/j.jhazmat.2013.09.057.

Kulkarni, S., Misra, C.S., Gupta, A., Ballal, A., Apte, S.K., 2016. Interaction of Uranium with Bacterial Cell Surfaces: Inferences from Phosphatase-Mediated Uranium Precipitation. Applied and Environmental Microbiology 82, 4965–4974. https://doi.org/10.1128/AEM.00728-16.

Lakaniemi, A.-M., Douglas, G.B., Kaksonen, A.H., 2019. Engineering and kinetic aspects of bacterial uranium reduction for the remediation of uranium contaminated environments. Journal of Hazardous Materials 371, 198–212. https://doi.org/10.1016/j.jhazmat.2019.02.074.

Latta, D.E., Mishra, B., Cook, R.E., Kemner, K.M., Boyanov, M.I., 2014. Stable U(IV) Complexes Form at High-Affinity Mineral Surface Sites. Environ. Sci. Technol. 48, 1683–1691. https://doi.org/10.1021/es4047389.

Li, X., Ding, C., Liao, J., Du, L., Sun, Q., Yang, J., Yang, Y., Zhang, D., Tang, J., Liu, N., 2017. Microbial reduction of uranium (VI) by *Bacillus* sp. dwc-2: A macroscopic and spectroscopic study. Journal of Environmental Sciences 53, 9–15. https://doi.org/10.1016/j.jes.2016.01.030.

Liang, X., Csetenyi, L., Gadd, G.M., 2016. Uranium bioprecipitation mediated by yeasts utilizing organic phosphorus substrates. Appl Microbiol Biotechnol 100, 5141–5151. https://doi.org/10.1007/s00253-016-7327-9.

López-Fernández, M., Cherkouk, A., Vilchez-Vargas, R., Jauregui, R., Pieper, D., Boon, N., Sanchez-Castro, I., Merroun, M.L., 2015. Bacterial Diversity in Bentonites, Engineered Barrier for Deep Geological Disposal of Radioactive Wastes. Microbial Ecology 70, 922–935. https://doi.org/10.1007/s00248-015-0630-7.

López-Fernández, M., Fernández-Sanfrancisco, O., Moreno-García, A., Martín-Sánchez, I., Sánchez-Castro, I., Merroun, M.L., 2014. Microbial communities in bentonite formations and their interactions with uranium. Applied Geochemistry 49, 77–86. https://doi.org/10.1016/j.apgeochem.2014.06.022.

Loreggian, L., Sorwat, J., Byrne, J.M., Kappler, A., Bernier-Latmani, R., 2020. Role of Iron Sulfide Phases in the Stability of Noncrystalline Tetravalent Uranium in

Sediments. Environ. Sci. Technol. 54, 4840–4846. https://doi.org/10.1021/acs.est.9b07186.
Luke, N.R., Sauberan, S.L., Russo, T.A., Beanan, J.M., Olson, R., Loehfelm, T.W., Cox, A. D., Michael, St. F., Vinogradov, E.V., Campagnari, A.A., 2010. Identification and Characterization of a Glycosyltransferase Involved in *Acinetobacter baumannii* Lipopolysaccharide Core Biosynthesis. Infection and Immunity 78, 2017–2023. https://doi.org/10.1128/IAI.00016-10.
Marquez, B., 2005. Bacterial efflux systems and efflux pumps inhibitors. Biochimie 87, 1137–1147. https://doi.org/10.1016/j.biochi.2005.04.012.
Merroun, M.L., Nedelkova, M., Ojeda, J.J., Reitz, T., Fernández, M.L., Arias, J.M., Romero-González, M., Selenska-Pobell, S., 2011. Bio-precipitation of uranium by two bacterial isolates recovered from extreme environments as estimated by potentiometric titration, TEM and X-ray absorption spectroscopic analyses. Journal of Hazardous Materials 197, 1–10. https://doi.org/10.1016/j.jhazmat.2011.09.049.
Merroun, M.L., Raff, J., Rossberg, A., Hennig, C., Reich, T., Selenska-Pobell, S., 2005. Complexation of Uranium by Cells and S-Layer Sheets of *Bacillus sphaericus* JG-A12. Appl. Environ. Microbiol. 71, 5532–5543. https://doi.org/10.1128/AEM.71.9.5532-5543.2005.
Merroun, M.L., Selenska-Pobell, S., 2008. Bacterial interactions with uranium: An environmental perspective. Journal of Contaminant Hydrology 102, 285–295. https://doi.org/10.1016/j.jconhyd.2008.09.019.
Metzger, L.E., Raetz, C.R.H., 2009. Purification and Characterization of the Lipid A Disaccharide Synthase (LpxB) from *Escherichia coli*, a Peripheral Membrane Protein. Biochemistry 48, 11559–11571. https://doi.org/10.1021/bi901750f.
Mitchell, A.M., Silhavy, T.J., 2019. Envelope stress responses: balancing damage repair and toxicity. Nature Reviews Microbiology 17, 417–428. https://doi.org/10.1038/s41579-019-0199-0.
Modi, N., Bárcena-Uribarri, I., Bains, M., Benz, R., Hancock, R.E.W., Kleinekathöfer, U., 2015. Tuning the Affinity of Anion Binding Sites in Porin Channels with Negatively Charged Residues: Molecular Details for OprP. ACS Chem. Biol. 10, 441–451. https://doi.org/10.1021/cb500399j.
Murphy, J., Riley, J.P., 1962. A modified single solution method for the determination of phosphate in natural waters. Analytica Chimica Acta 27, 31–36. https://doi.org/10.1016/S0003-2670(00)88444-5.
Murahari, P., Anishetty, S., Pennathur, G., 2013. Understanding the lid movements of LolA in *Escherichia coli* using molecular dynamics simulation and in silico point mutation. Computational Biology and Chemistry 47, 71–80. https://doi.org/10.1016/j.compbiolchem.2013.06.005.
Newsome, L., Morris, K., Lloyd, J.R., 2014. The biogeochemistry and bioremediation of uranium and other priority radionuclides. Chemical Geology 363, 164–184. https://doi.org/10.1016/j.chemgeo.2013.10.034.
Newsome, L., Morris, K., Trivedi, D., Bewsher, A., Lloyd, J.R., 2015. Biostimulation by Glycerol Phosphate to Precipitate Recalcitrant Uranium(IV) Phosphate. Environ. Sci. Technol. 49, 11070–11078. https://doi.org/10.1021/acs.est.5b02042.
Nies, D.H., 2003. Efflux-mediated heavy metal resistance in prokaryotes. FEMS Microbiology Reviews 27, 313–339. https://doi.org/10.1016/S0168-6445(03)00048-2.
Nilgiriwala, K.S., Alahari, A., Rao, A.S., Apte, S.K., 2008. Cloning and Overexpression of Alkaline Phosphatase PhoK from *Sphingomonas* sp. Strain BSAR-1 for Bioprecipitation of Uranium from Alkaline Solutions. Applied and Environmental Microbiology 74, 5516–5523. https://doi.org/10.1128/AEM.00107-08.
Nilsson, G., Belasco, J.G., Cohen, S.N., von Gabain, A., 1984. Growth-rate dependent regulation of mRNA stability in *Escherichia coli*. Nature 312, 75–77. https://doi.org/10.1038/312075a0.
Orellana, R., Hixson, K.K., Murphy, S., Mester, T., Sharma, M.L., Lipton, M.S., Lovley, D. R., 2014. Proteome of *Geobacter sulfurreducens* in the presence of U(VI). Microbiology 160, 2607–2617. https://doi.org/10.1099/mic.0.081398-0.
Park, D.M., Jiao, Y., 2014. Modulation of Medium pH by *Caulobacter crescentus* Facilitates Recovery from Uranium-Induced Growth Arrest. Appl. Environ. Microbiol. 80, 5680–5688. https://doi.org/10.1128/AEM.01294-14.
Rosenfeld, Y., Shai, Y., 2006. Lipopolysaccharide (Endotoxin)-host defense antibacterial peptides interactions: Role in bacterial resistance and prevention of sepsis. Biochimica et Biophysica Acta (BBA) - Biomembranes 1758, 1513–1522. https://doi.org/10.1016/j.bbamem.2006.05.017.
Salome, K.R., Beazley, M.J., Webb, S.M., Sobecky, P.A., Taillefert, M., 2017. Biomineralization of U(VI) phosphate promoted by microbially-mediated phytate hydrolysis in contaminated soils. Geochimica et Cosmochimica Acta 197, 27–42. https://doi.org/10.1016/j.gca.2016.10.008.
Sánchez-Castro, I., Bakkali, M., Merroun, M.L., 2017a. Draft Genome Sequence of *Stenotrophomonas bentonitica* BII-R7 ^{T}, a Selenite-Reducing Bacterium Isolated from Spanish Bentonites. Genome Announcements 5. https://doi.org/10.1128/genomeA.00719-17.
Sánchez-Castro, I., Ruiz-Fresneda, M.A., Bakkali, M., Kämpfer, P., Glaeser, S.P., Busse, H. J., López-Fernández, M., Martínez-Rodríguez, P., Merroun, M.L., 2017b. *Stenotrophomonas bentonitica* sp. nov., isolated from bentonite formations. International Journal of Systematic and Evolutionary Microbiology 67, 2779–2786. https://doi.org/10.1099/ijsem.0.002016.
Santos-Beneit, F., 2015. The Pho regulon: a huge regulatory network in bacteria. Front. Microbiol. 6. https://doi.org/10.3389/fmicb.2015.00402.
Schmid, J., Heider, D., Wendel, N.J., Sperl, N., Sieber, V., 2016. Bacterial Glycosyltransferases: Challenges and Opportunities of a Highly Diverse Enzyme Class Toward Tailoring Natural Products. Front. Microbiol. 7. https://doi.org/10.3389/fmicb.2016.00182.
Selvakumar, R., Ramadoss, G., Menon, Mridula P., Rajendran, K., Thavamani, P., Naidu, Ravi, Megharaj, M., 2018. Challenges and complexities in remediation of uranium contaminated soils: A review. Journal of Environmental Radioactivity 192, 592–603. https://doi.org/10.1016/j.jenvrad.2018.02.018.
Sivaswamy, V., Boyanov, M.I., Peyton, B.M., Viamajala, S., Gerlach, R., Apel, W.A., Sani, R.K., Dohnalkova, A., Kemner, K.M., Borch, T., 2011. Multiple mechanisms of uranium immobilization by *Cellulomonas* sp. strain ES6. Biotechnology and Bioengineering 108, 264–276. https://doi.org/10.1002/bit.22956.
Skouri-Panet, F., Benzerara, K., Cosmidis, J., Férard, C., Caumes, G., De Luca, G., Heulin, T., Duprat, E., 2018. In Vitro and in Silico Evidence of Phosphatase Diversity in the Biomineralizing Bacterium *Ramlibacter tataouinensis*. Frontiers in Microbiology 8. https://doi.org/10.3389/fmicb.2017.02592.
Slobodkin, A.I., Sokolova, T.G., Lysenko, A.M., Wiegel, J., 2006. Reclassification of Thermoterrabacterium ferrireducens as *Carboxydothermus ferrireducens* comb. nov., and emended description of the genus *Carboxydothermus*. International Journal of Systematic and Evolutionary Microbiology 56, 2349–2351. https://doi.org/10.1099/ijs.0.64503-0.
Smith, S.G.J., Mahon, V., Lambert, M.A., Fagan, R.P., 2007. A molecular Swiss army knife: OmpA structure, function and expression. FEMS Microbiology Letters 273, 1–11. https://doi.org/10.1111/j.1574-6968.2007.00778.x.
Sonntag, I., Schwarz, H., Hirota, Y., Henning, U., 1978. Cell envelope and shape of *Escherichia coli*: multiple mutants missing the outer membrane lipoprotein and other major outer membrane proteins. Journal of Bacteriology 136, 280–285. https://doi.org/10.1128/JB.136.1.280-285.1978.
Sowmya, S., Rekha, P.D., Arun, A.B., 2014. Uranium(VI) bioprecipitation mediated by a phosphate solubilizing Acinetobacter sp. YU-SS-SB-29 isolated from a high natural background radiation site. International Biodeterioration & Biodegradation 94, 134–140. https://doi.org/10.1016/j.ibiod.2014.07.009.
Suzuki, Y., Banfield, J.F., 2004. Resistance to, and Accumulation of, Uranium by Bacteria from a Uranium-Contaminated Site. Geomicrobiology Journal 21, 113–121. https://doi.org/10.1080/01490450490266361.
Tavares-Carreón, F., Fathy Mohamed, Y., Andrade, A., Valvano, M.A., 2015. ArnT proteins that catalyze the glycosylation of lipopolysaccharide share common features with bacterial *N* -oligosaccharyltransferases. Glycobiology, cwv095. https://doi.org/10.1093/glycob/cwv095.
Theodorakopoulos, N., Chapon, V., Coppin, F., Floriani, M., Vercouter, T., Sergeant, C., Camilleri, V., Berthomieu, C., Février, L., 2015. Use of combined microscopic and spectroscopic techniques to reveal interactions between uranium and *Microbacterium* sp. A9, a strain isolated from the Chernobyl exclusion zone. Journal of Hazardous Materials 285, 285–293. https://doi.org/10.1016/j.jhazmat.2014.12.018.
Troxell, B., Hassan, H.M., 2013. Transcriptional regulation by Ferric Uptake Regulator (Fur) in pathogenic bacteria. Front. Cell. Infect. Microbiol. 3. https://doi.org/10.3389/fcimb.2013.00059.
Tu, H., Yuan, G., Zhao, C., Liu, J., Li, F., Yang, J., Liao, J., Yang, Y., Liu, N., 2019. U-phosphate biomineralization induced by *Bacillus* sp. dw-2 in the presence of organic acids. Nuclear Engineering and Technology 51, 1322–1332. https://doi.org/10.1016/j.net.2019.03.002.
Verissimo, A.F., Daldal, F., 2014. Cytochrome c biogenesis System I: An intricate process catalyzed by a maturase supercomplex. Biochimica et Biophysica Acta (BBA) - Bioenergetics 1837, 989–998. https://doi.org/10.1016/j.bbabio.2014.03.003.
Wang, G., Liu, J., Wang, X., Xie, Z., Deng, N., 2009. Adsorption of uranium (VI) from aqueous solution onto cross-linked chitosan. Journal of Hazardous Materials 168, 1053–1058. https://doi.org/10.1016/j.jhazmat.2009.02.157.
Wang, L., Xiao, S., Chen, X., Chen, S., Wang, S., Wang, C., Tang, Y., Dong, F., 2019. ytiB and ythA Genes Reduce the Uranium Removal Capacity of *Bacillus atrophaeus*. IJMS 20, 1766. https://doi.org/10.3390/ijms20071766.
Wang, P., Guo, Q., Ma, Y., Li, S., Lu, X., Zhang, X., Ma, P., 2015. DegQ regulates the production of fengycins and biofilm formation of the biocontrol agent *Bacillus subtilis* NCD-2. Microbiol. Res. 178, 42–50. https://doi.org/10.1016/j.micres.2015.06.006.
Wang, Y., 2002. The function of OmpA in Escherichia coli. Biochem. Biophys. Res. Commun. 292, 396–401. https://doi.org/10.1006/bbrc.2002.6657.
Wei, Y., Chen, Z., Song, H., Zhang, J., Lin, Z., Dang, Z., Deng, H., 2019. The immobilization mechanism of U(VI) induced by Bacillus thuringiensis 016 and the effects of coexisting ions. Biochemical Engineering Journal 144, 57–63. https://doi.org/10.1016/j.bej.2019.01.013.
Xu, R., Wu, K., Han, H., Ling, Z., Chen, Z., Liu, P., xiong, J., Tian, F., Zafar, Y., Malik, K., Li, X., 2018. Co-expression of YieF and PhoN in *Deinococcus radiodurans* R1 improves uranium bioprecipitation by reducing chromium interference. Chemosphere 211, 1156–1165. https://doi.org/10.1016/j.chemosphere.2018.08.061.
Yang, T., Chen, M.-L., Wang, J.-H., 2015. Genetic and chemical modification of cells for selective separation and analysis of heavy metals of biological or environmental significance. TrAC Trends in Analytical Chemistry 66, 90–102. https://doi.org/10.1016/j.trac.2014.11.016.
Yung, M.C., Jiao, Y., 2014. Biomineralization of Uranium by PhoY Phosphatase Activity Aids Cell Survival in Caulobacter crescentus. Applied and Environmental Microbiology 80, 4795–4804. https://doi.org/10.1128/AEM.01050-14.
Yung, M.C., Ma, J., Salemi, M.R., Phinney, B.S., Bowman, G.R., Jiao, Y., 2014. Shotgun Proteomic Analysis Unveils Survival and Detoxification Strategies by *Caulobacter*

crescentus during Exposure to Uranium, Chromium, and Cadmium. J. Proteome Res. 13, 1833–1847. https://doi.org/10.1021/pr400880s.

Yung, M.C., Park, D.M., Overton, K.W., Blow, M.J., Hoover, C.A., Smit, J., Murray, S.R., Ricci, D.P., Christen, B., Bowman, G.R., Jiao, Y., 2015. Transposon Mutagenesis Paired with Deep Sequencing of Caulobacter crescentus under Uranium Stress Reveals Genes Essential for Detoxification and Stress Tolerance. Journal of Bacteriology 197, 3160–3172. https://doi.org/10.1128/JB.00382-15.

Zhang, J., Song, H., Chen, Z., Liu, S., Wei, Y., Huang, J., Guo, C., Dang, Z., Lin, Z., 2018. Biomineralization mechanism of U(VI) induced by Bacillus cereus 12-2: The role of functional groups and enzymes. Chemosphere 206, 682–692. https://doi.org/10.1016/j.chemosphere.2018.04.181.